NASA Contractor Report 181664

Expanded Envelope Concepts for Aircraft Control-Element Failure Detection and Identification

Jerold L. Weiss
John Y. Hsu

ALPHATECH, Inc.
Burlington, Massachusetts

June 1988

Prepared for
Langley Research Center
Under Contract NAS1-18004

NASA
National Aeronautics and
Space Administration

Langley Research Center
Hampton, Virginia 23665

NASA Contractor Report 181664

Expanded Envelope Concepts for Aircraft Control-Element Failure Detection and Identification

Jerold L. Weiss
John Y. Hsu

ALPHATECH, Inc.
Burlington, Massachusetts

June 1988

Prepared for
Langley Research Center
Under Contract NAS1-18004

National Aeronautics and
Space Administration

Langley Research Center
Hampton, Virginia 23665

NASA Contractor Report 181664

TR-378

EXPANDED ENVELOPE CONCEPTS FOR AIRCRAFT CONTROL-ELEMENT FAILURE DETECTION AND IDENTIFICATION

June 1988

By:

Jerold L. Weiss
John Y. Hsu

Submitted to:

W.T. Bundick
NASA Langley Research Center
Hamptom, VA

Contract No. NAS1-18004

ALPHATECH, Inc.
111 Middlesex Turnpike
Burlington, Massachusetts 01803
(617) 273-3388

CONTENTS

CONTENTS (continued)

SECTION 1

INTRODUCTION

This report presents the results of Task 5 for contract NAS1-18004, sponsored by the NASA Langley Research Center. The purpose of this work has been to develop and demonstrate methods of design and analysis of control-element failure detection and isolation (FDI) algorithms for restructurable flight control systems. This work was coupled with contract NAS1-17411 in which control restructuring methods were developed. Several reports document these efforts ([1]-[3]*). Reference [1] details automatic control design procedures for the restructurable control problem and reference [2] details the FDI methods that play a key role in enabling the effectiveness of the control redesign procedures. Reference [3] documents a preliminary integration of the control redesign and FDI concepts into Fortran-77 subroutine that were then used as the flight control module in NASA's B-737 simulation. These efforts all dealt with operation of the aircraft at a single flight condition. Promising results at a single flight condition lead to the effort reported herein, in which expanded envelopes of operation are considered.

The purpose of this effort was to develop and demonstrate concepts for expanding the envelope of the FDI algorithms that detect and isolate "aircraft-path" failures. An "aircraft path" failure is defined as a control element failure based on the analytic redundancy contained in the models and measurements associated with force and moment relationships. These failures are the most difficult to detect and isolate since analytical relationships between dissimilar sensors ("analytic-redundancy") must be used. In particular, aerodynamic force and moment balance equations that relate measurements of control deflection, angular rates, and relative wind velocities to translational and rotational accelerations are used to compare actual aircraft motion with expected motion and to detect and identify peculiarities of any discrepancy. Because aircraft-path FDI must

* References are indicated by numbers in square brackets; the list appears at the end of the main body of this report.

rely on force and moment balance models, there is a natural tradeoff between the accuracy of these models and the ability to detect and isolate failures. For single flight condition operation, we developed design and analysis methods to deal with this "robustness" problem. When the departure from the single flight condition is significant, however, it is not possible to obtain adequate performance (i.e., both low false alarm and missed detection probabilities) without some form of adaptation. This report deals with those adaptations.

While previous work was applied to models of the B-737 aircraft, this work was applied to a high performance fighter aircraft model (the AFTI/F-16) since such aircraft are likely to have more stringent restructurable control requirements [1]. The basic methods, however, are valid for transport as well as fighter aircraft.

1.1 SUMMARY

All FDI methods can be decomposed into two major elements; residual generation and decision-making. In [2], we explicitly considered the design of each of these elements separately in order to better understand and compensate for the effects of many non-idealized factors. This effort deals with adaptation mechanisms for expanded envelope operation in the same way.

For residual generation, adaptation requirements are interpreted as the need for accurate, large-motion models, over a broad range of velocity and altitude conditions (in-flight model identification was initially considered as a method of residual adaptation but was rejected for several reasons; see Section 2). For decision-making, adaptation may require modifications to the filtering operations, thresholds, and projection vectors that define the various hypothesis tests performed in the decision mechanism.

Methods of obtaining and evaluating residual generation and decisionmaking designs in an expanded envelope context have been developed for this project. In addition, we have demonstrated the application of the residual generation ideas to a high-performance fighter by developing "adaptive" and single flight condition residuals for the AFTI/F-16 and simulating their behavior under a variety of maneuvers using the results of NASA's F-16 simulation.

SECTION 2

DESIGN METHODS FOR EXPANDED ENVELOPE OPERATION RESIDUAL GENERATION

In the next two sections we discuss several issues that must be addressed in expanding the envelope of operation of the FDI algorithm developed in [2]. Although we consider this algorithm explicitly, many of these issues apply to any FDI algorithm. Residual generation and decision mechanism issues are addressed separately (residual generation in this section and decisionmaking in Section 3), although, as often stated, the performance capabilities of one affects the performance requirements of the other. For both FDI processes we discuss when the need for envelope-expanding adaptation arises and determine the factors that might affect this need. We then present various methods that can be used in the design of adaptation mechanisms.

2.1 DESIGN ISSUES

The generation of good residuals for use in any decision making process requires, ultimately, high fidelity models of the aircraft. Although the concept of "adaptation" is sometimes taken to mean on-line "learning" (of the aircraft models for example), for our purposes the term adaptation refers to a model "scheduling" concept. The primary reason for this view is the inherent problems associated with learning types of adaptation within an FDI context; the problem being the adaptation (of aircraft models in our case) to the effects (of the failure) that need to be detected. While such adaptation could ultimately provide the information required for reconfiguration (e.g., new aircraft models), it obscures the detection problem, which must make high fidelity decisions in very short amounts of time (an order of magnitude faster than what is usually required for accurate model adaptation [4]).

The attainment of truly high fidelity aircraft models over a wide range of operating conditions (various dynamic pressure and maneuver conditions) is a difficult problem and, in principle, could involve excessive physical modeling of static and dynamic aerodynamic behavior as well as validation with wind tunnel and flight test results. Even with such an excessive effort, variations amongst aircraft of the same type and variations of a single aircraft over time are typically ignored. However, the accuracy requirements for the control element FDI problem are such that simple models based on static aircraft characteristics will be sufficient for nearly all flight conditions and where they are not (e.g., during transient/dynamic airflow conditions) adequate compensation of the decision making process can be made.

The keys to the development of adequate aircraft models over a wide range of operating conditions are as follows;

1. Good physical understanding of aerodynamic effects, and
2. A means of assessing the quality of any proposed model.

The need for physical intuition comes about because of the size and number of effects that must be modeled. For example, a single residual may be a function of 5 to 10 (measurable) variables. To model the relationship between the variables (e.g., with a power series) without some knowledge of how these variables interact and what types of nonlinearities are possible would require an unrealistic number of terms (many of which may end up being insignificant) and a possible over-fitting of the model, [5]. Thus, physical intuition allows proper model forms to be chosen more easily. For this project, adequate time was not available for a full investigation of nonlinear and full-envelope modeling issues. Therefore, our approach was to examine and compare a variety of nonlinear aerodynamic models and deduce as much as possible about the possible nonlinearities and interactions amongst variables.

Once a model is (or models are) chosen, evaluation in terms that relate directly to the residual generation process is necessary. This is at least as important if not more important, than developing a good model since accurate characterization of uncertainty leads to accurate

performance prediction. As discussed in [2], performance of FDI algorithms depends , in part, on the power spectral density of the residuals. This PSD is used to design and evaluate the decision mechanism in terms of detectable and isolatable failure magnitudes. Thus, the ultimate measure of model quality is the performance of the decision mechanism that uses the corresponding model for residual generation. While this is the ultimate measure, its computation could be quite involved; including, as it does, a complete decisionmaking design. Therefore, simpler measures are sought. For this project, we will assume that the filtering requirements for each statistical test in the decision mechanism are the same, and can be determined (roughly) before residual generation models are formed. Furthermore, we will again assume that two types of errors arise, low-frequency "in-band" errors that are unaffected by filtering, and sensor noise, whose effect is reduced by filtering. As a result, the use of a predicted value for the variance of each residual after filtering is proposed as a measure of model quality.

The three primary issues that must be considered in building an aircraft model for residual generation are:

1. Model fidelity,
2. Model simplicity, and
3. The ability to predict model accuracy in terms of actual aircraft performance.

Most aircraft development programs go through several phases of modeling in which higher-fidelity models are built. While it is tempting to use the latest (and presumably best) models for residual generation, the final model that comes out of a full-scale flight test tends to be very complex (including table look-up functions and flight-test correction factors). For residual generation, the simplification of such a model is required for real time operation. Of course, with simplification comes errors. Thus, in characterizing the quality of the models inaccuracies between the best model and its simplification, as well as inaccuracies between the best model and the real aircraft, should be taken into account. The former characterization

occurs naturally in the model simplification process. The latter issue is more difficult and needs to be addressed in future work.

The simplification of a high fidelity aerodynamic aircraft model for residual generation purposes is essentially the same as any model simplification or data-analysis procedure. The six steps in this process are:

1. Determination of potential nonlinearities and interactions from knowledge of aerodynamic concepts,
2. Generation of aerodynamic coefficient values as a function of important "independent" (and measurable) variables,
3. Plotting of this data to examine anticipated nonlinearities and interactions,
4. Proposal of a series of analytic model forms for use in residual generation,
5. Fitting of each model to the data using a regression analysis, and
6. Selection of the best model according to a prediction of the variance of the filtered residual.

Steps 4-6 can be accomplished in a variety of ways (e.g., "all-subset regression", "backward elimination", and "stepwise regression"; see [5]). In all of these methods, it is assumed that the dependent variable (the aerodynamic coefficient) is a sum of terms involving the independent variables. The possible terms must be spelled out ahead of time and is the most difficult part of any of these methods. This is where steps 1 and 3 (especially plotting the data) are needed. For example, potential nonlinear effects that would be expected [e.g., see [6]) include:

1. Lift-Curve slope for wings varying as $\frac{1}{\sqrt{(1-M^2)}}$.
2. Increases in α (below $\alpha_{crit.}$) can increase the roll, yaw, and sideslip effectiveness on lateral coefficients.
3. Reductions in control effectiveness can be expected at high local angles of attack.
4. Effectiveness of trailing edge surfaces are proportional to local angles of attack.
5. Drag is affected by lift (i.e., drag polars).
6. Small effects of sideslip on lift can be expected.

7. Various control nonlinearities are likely.

8. Trailing edge wing surfaces are likely to interact with the effects of horizontal tail surfaces.

9. Pitch effectiveness can be proportional to higher powers of lift (e.g., CL^2, CL^3).

10. Angle-of-attack rate can affect longitudinal coefficients.

11. The effectiveness of trailing-edge surfaces are proportional to $\frac{1}{\sqrt{(1-M^2)}}$.

Various specific effects for individual models can also be derived. For example, for the rolling moment model, we would expect an iteration between α and β since the effect of β on roll is dependent on wing and horizontal-tail lift, which is in turn dependent on α. The magnitude of the interaction depends on the amount of wing sweep and dihedral/anhedral of the wings and horizontal tail. The lift on the wings and horizontal-tail are also influenced by deflection of the flaperons, thereby giving rise to a possible interaction between β and flaperon deflection. Nonlinearities in β might be expected at high sideslip angles as a result of the transition from laminar to turbulent flow over the fuselage. Finally, interactions between β and canard deflection might be expected since the snowplow configuration presents an asymmetrical profile to side wind components and the location of the canards is such that rolling moments may result.

2.2 DESIGN METHODS

As discussed above, the development of high-fidelity, full-envelope, aero-models requires that all important nonlinearities be modeled. We have divided these nonlinear effects into two categories; 1) large-amplitude effects, and 2) flight-condition effects. The large-amplitude effects are due to large perturbational changes in aircraft velocities (magnitude and direction of translational and rotational velocities) at a single flight-condition (Mach, altitude). Large-amplitude effects require nonlinear models mainly because of the changes in lift distributions on the various components (wings, body, horizontal tail, etc.) of the aircraft (they do not all change equally). Changing flight-conditions cause changes in the "scaling" of the nondimensional coefficients (linearly with dynamic pressure; hence a nonlinear multiplicative

model) as well as changes in the nondimensional coefficients themselves. The latter effect is due to changing lift characteristics as described in [1] and due to changes in the geometry of the aircraft due to static flex characteristics. For this project, we will concentrate on developing analytical models for large-amplitude effects. Expansion of the envelope to incorporate a wider range of flight-conditions will take the form of a scheduling of the "parameters" of several single flight-condition models.

As discussed previously, the first step in developing models for residual generation is to determine the form of the models from basic aerodynamic principles, Towards this end, two forms have been developed. The first form is based on a simple generalization of the so-called "panel" or "component build-up" method. It involves a simple model for the lift and drag due to each component (wings, body, horizontal tail, etc.) of the aircraft as a function of the local relative wind vector, the panel's "configuration" (e.g., changing camber due to flaps), and possible changes in the relative wind vector due to interference effects. The second form is a generalization of the linear models commonly used in flight control design and is therefore called a quasi-linear method. In this modelling method, the nondimensional "derivatives" are functions of variables that would be expected to cause them to change for physical reasons. Both methods are discussed below.

2.2.1 Panel Method Models

The basic idea of the panel method is that each panel or component of the aircraft generates a lift and drag vector whose magnitude and direction are largely determined by the magnitude and direction of the local relative wind. This is a common method of aircraft modelling [1], [2] and we use it here to provide a simple model form whose specific parameters can be identified from an aero-package.

Let L_i and D_i represent the (dimensional) lift and drag force vectors (expressed in a body-referenced coordinate system) on the i-th panel of the aircraft. We assume [6] that each vector is applied to the aircraft at some average location, r_i, that the drag vector is applied

parallel to the relative wind vector, V_i, and the lift vector is orthogonal to V_i and a unit span vector, e_i^b, for the i-th panel. From these assumptions it is easy to see that each panel generates a portion of the total force and moment on the aircraft (at the center of gravity). The total body-referenced force on the aircraft is

$$F = \sum_i L_i + D_i \tag{2-1}$$

The total moment on the aircraft is

$$M = \sum_i r_i \times L_i + r_i \times D_i \tag{2-2}$$

The magnitude of lift on each panel is modeled as a function of V_i, an interference variable σ_i (e.g., downwash angle for the horizontal tail), and any configuration variables (e.g., flap deflection for the wings, rudder deflection for the vertical tail panel). For a wide range of local angles of attack, each panel can be adequately modeled by [6]

$$| L_i | = 1/2\, \rho\, (U_i)^2 \, (L_i^o + K_\alpha^i \, (W_i/U_i - \sigma_i) + K_\delta^i \, \delta_i), \tag{2-3}$$

where U_i is the local forward velocity (i.e., the projection of V_i onto a unit chord-vector, e_i^c, for the i-th panel), W_i is the local downward velocity (i.e., the projection of V_i onto a unit vector that is orthogonal to e_i^c and e_i^b), L_i^o is the basic panel lift coefficient for the desired flight condition, W_i/U_i is an approximation to the local angle of attack, ρ is the atmospheric density, and δ_i is a "configuration" variable (such as trailing/leading edge wing flaps). The interference variable, σ_i , can also be a function of other parameters and is the least understood part of the panel model. Also, note that for some panels (e.g., canards) the projections of V_i onto span- and chord- referenced directions will change (e.g., as a function of canard deflection) since these vectors can be changed.

The magnitude of the drag due to each panel is then assumed to be computed from the drag-polar relationship [6]

$$|D_i| = D_i^o + K_{DL} |L_i|^2 \tag{2-4}$$

The local relative wind vector, V_i, is computed from [7]

$$V_i = V_{rw} + \omega \times r_i, \tag{2-5}$$

where V_{rw} is the overall or average relative wind vector on the aircraft, and ω is the body-referenced angular velocity vector.

These equations reduce the modeling problem to one of identifying a few basic quantities: r_i, L_i^o, K_α^i, K_δ^i, e_i^c, and e_i^b. Knowledge of the form of these equations should also allow large reductions in the amount of data needed to identify the desired quantities. For example, the values of L_i^o, K_α^i, K_δ^i can be determined solely from force relationships at $\omega = 0$. Unfortunately, there are some drawbacks to this approach. First, the resulting model is not particularly efficient computationally. Many "small" effects that perhaps could be ignored are modeled through these relationships. It is also possible that the addition of "small" effects can cause deterioration of the quality of the resulting residuals, due to the addition of sensor noise. These situations are particularly difficult to identify with this model. Also, while the assumption about the directions of lift and drag on each panel are fairly standard, it is not clear how accurate this assumption will be in terms of the residual generation problem. Finally, the model ignores some potentially important effects such as the movement of the center of pressure (essentially r_i) at a single flight condition. For these reasons, this method is not considered further.

2.2.2 Quasi-Linear Models

This method of modeling is also common in flight control applications. The basic idea is to assume a model for the non-dimensional coefficients of the form,

$$C_\zeta = \sum_i C_{\zeta\psi}{}^i \psi^i \tag{2-6}$$

where ξ = x, y, z, l, m, or n, the ψ^i are the measurable quantities that are likely to affect C_ξ and the $C_{\xi\psi^i}$ are modeled as functions of the ψ^i likely to affect them (still at a single flight condition). We use physical knowledge about aerodynamics to postulate the important terms in the above equation as well as the quantities that are likely to affect the "derivatives", $C_{\xi\psi^i}$. For example, for the F-16 we have developed the roll-coefficient model

$$
\begin{aligned}
C_l = \quad & \\
& C_{l\_r}(\alpha)\, r + \\
& C_{l\_p}(\alpha)\, p + \\
& C_{l\_\beta}(\alpha, dfc, dsp, \beta)\, \beta + \\
& C_{l\_dfa}(\alpha, dfc, dfa)\, dfa + \\
& C_{l\_dhta}(\alpha, dfc, dfa)\, dhta + \\
& C_{l\_dr}(\alpha, dfc, dr)\, dr + \\
& C_{l\_dvc}(\alpha, \beta, dvc)\, dvc, \qquad (2\text{-}7)
\end{aligned}
$$

where

α = aircraft angle of attack,

β = aircraft sideslip angle,

dfc = collective flaperon deflection,

dfa = asymmetric (differential) flaperon deflection,

dhta = asymmetric horizontal tail deflection,

dvc = parallel/vertical canard deflection,

dsp = snowplow/horizontal canard deflection,

dr = rudder deflection,

The terms in the roll-coefficient expansion are the same as those that appear in a linear model. The variation of the derivatives with other variables takes into account various physical effects.

For example, C_{l_β} varies with α because C_{l_β} is partly due to wing sweep. The effect of wing sweep, however, increases as the wing lift increases [6], which increases with α. Note that the anhedral of the vertical tail and canards also contribute to C_{l_β} with opposite sign (to the sweep effect). This effect also increases with lift and hence α. The overall relationship between C_{l_β} and α is indeterminate since the relative contributions of these physical phenomena are unknown. However, it is clear that C_{l_β} could be a function of α and hence we should attempt to characterize it for residual generation. Similarly, C_{l_β} is a function of (dfc) because of its effect on the lift of the wing, thereby affecting the wing sweep effect. The dependence on (dsp) is due to the asymmetric profile to side wind components presented by the (dsp) configuration and the location of the canards below the x body axis; and the dependence on β indicates that we expect decreases in C_{l_β} at large sideslip angles due to separation (i.e., departure from laminar flow).

The advantage of the quasi-linear approach is that the resulting models are significantly simpler than any that could be proposed without knowledge of important aerodynamic effects. This approach also reduces the effort associated with identifying the parameters of the model since each term can be identified independently (i.e., set all variables to zero except the one corresponding to the derivative being examined). For example, Fig. 2-1 shows a plot of C_{l_β} vs. β for various values of α. This plot suggests that for small sideslip angles, a model of the form $C_{l\_\beta} = K (\alpha - \alpha_0)^2$ may be appropriate. For larger values of β, some nonlinearity in β needs to be considered. Also, the effects of dfc and dsp need to be examined. Because each derivative is only a function of a few variables, the analysis of important nonlinearities and interactions amongst variables is substantially easier than if we attempted to formulate a model without any predetermined structure such as the quasi-linear form. It should also be clear that the analysis of "small" effects and their ultimate impact on the residual generation process is simpler using the quasi-linear model.

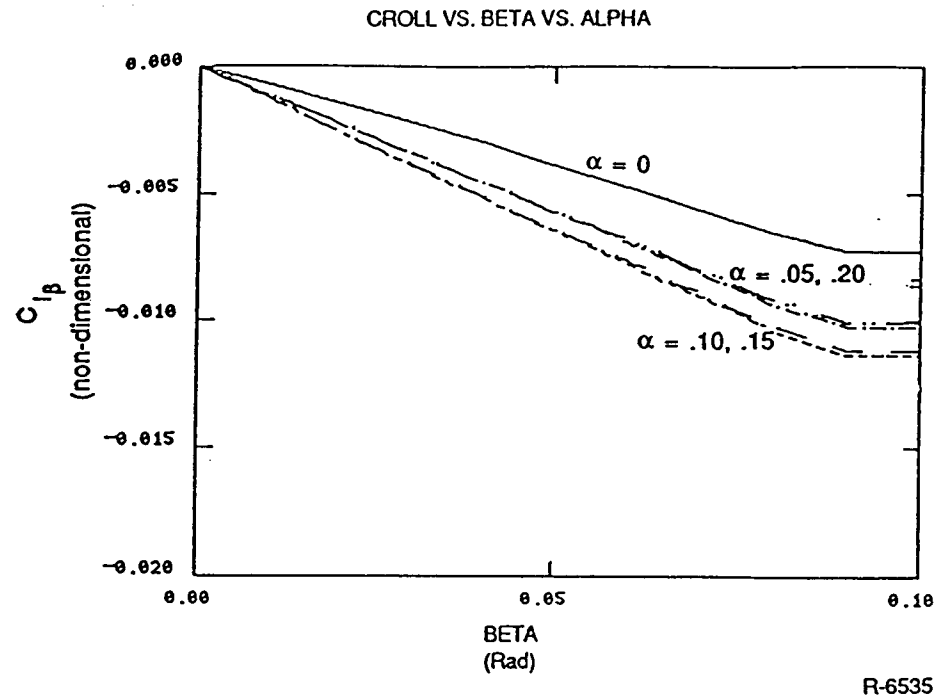

Figure 2-1a. Croll vs. Beta vs. Alpha.

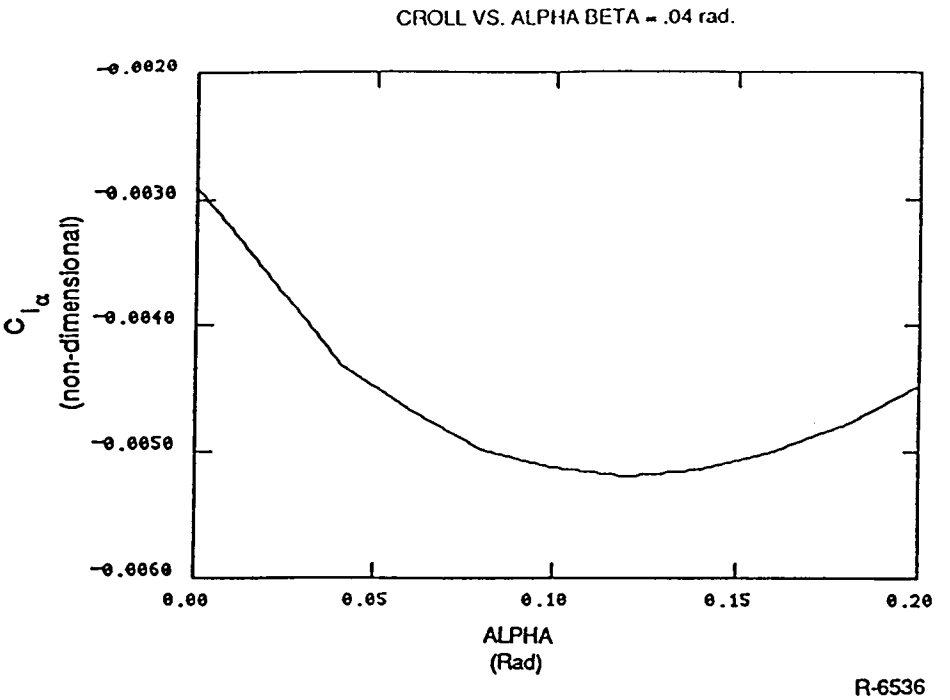

Figure 2-1b. Croll vs. Alpha vs. Beta (b = .04 Rad.).

2.2.3 Regression Analysis for "Linear" Models

The quasi-linear models described in subsection 2.2.2 are frequently reduced to models that are linear in an unknown set of parameters (e.g., a polynomial model [8]; note that linearity in the "independent" variables of the model is not implied). For such models, sophisticated iterative regression analyses have been developed (stepwise, backward elimination, etc., see [5]). With such iterative methods, models are iteratively proposed and evaluated until the "best" model is obtained. The sophistication of these methods involves the use of calculations as part of each regression that help select the next course of action (as opposed to more general search strategies that require full model fitting for alternative steps).

Some controversy as to the definition of a "best" model exists, however. This controversy stems from the fact that the ultimate use of the model to be found varies from application to application. Some general rules are applicable in many circumstances. For example, to paraphrase [8], if two models have similar error characteristics, the one with the fewer terms is better. For the residual generation problem, this makes sense since extra terms imply extra error due to sensor noise (when residuals are actually formed). However, since this is the primary reason for rejecting models with large terms, it is desirable to formulate and solve a regression problem that deals with the sensor noise problem directly. This is done in the following.

The regression problem we wish to solve assumes that the residual equation is given by,

$$\nu = y^m - (a_1 x_1^m + a_2 x_2^m + \dots) \qquad (2\text{-}8)$$

where the x_i^m's are terms that involve measurable quantities (including nonlinear terms), the a_i's are coefficients to be determined, and y^m is the measurement (of acceleration) that is to be predicted. For example, the model for lateral acceleration might be expressed as :

$$\nu_y = a_y^m - (a_{y\_\beta}\, \beta^m + a_{y\_p}\, p^m + a_{y\_p\alpha}\, p^m \alpha^m + \dots) \qquad (2\text{-}9)$$

The residual produced within the FDI system from this equation will be nonzero during unfailed conditions due to model error and due to sensor noise.

We now define sensor disturbances that are used to predict the size of the effect of sensor errors on the residuals. Let,

$$y^m = y + n_y \tag{2-10a}$$

and,

$$x_i^m = x_i + n_{x\_i} \ . \tag{2-10b}$$

The characteristics of the terms n_y and n_{x_i} are determined by the properties of the individual sensors used in the residual generation process. In Eq. 2-9 the lateral acceleration noise n_{ay} as well as noises on sensors of β, α, and p are considered independent zero-mean white Gaussian processes. The characteristics of n_y and the corresponding n_{x_i} 's are then uniquely determined. In this example, they are all trivial except for the αp term which has

$$n_{\alpha p} = (p\, n_\alpha + \alpha\, n_p + n_\alpha n_p) \quad . \tag{2-11}$$

Note that while the individual sensor errors may be assumed to be independent, there may still be correlation between n_{x_i} and n_{x_j} due to nonlinearities in the measurable quantities.

Using the above definitions, the covariance of the residual is expressed as :

$$E\{ \nu^t \nu\} = E\{(y - \underline{a}^t \underline{x})^t (y - \underline{a}^t \underline{x})\} + \sigma_y^2 + \underline{a}^t \Sigma \underline{a} \tag{2-12}$$

where, $\underline{a}^t = (a_1, a_2, \ldots)$, $\underline{x}^t = (x_1, x_2, \ldots)$, $\sigma_y^2 = E\{ n_y^2\}$, and $[\Sigma]_{ij} = E\{ n_{x\_i}\, n_{x\_j} \}$. Now, the first term in Eq. 2-12 represents the modeling error between the quasi-linear model and the actual aircraft. If we assume that this error is statistically similar to the model simplification error, then Eq. 2-12 can be rewritten as,

$$E\{ \nu^t \nu\} = \frac{1}{N-1} \ (\underline{y} - \underline{X}\,\underline{a})^t \ (\underline{y} - \underline{X}\,\underline{a}) + \sigma_y^2 + \underline{a}^t \Sigma \underline{a} \tag{2-13}$$

where N = number of data points, $[y]_i$ = the i-th sample of y from the aero-data package, and $[X]_{ij}$ = i-th sample of x_j from the aero-data. Now, since Σ can be calculated from knowledge of sensor noises and the nonlinearities involved in each x_i, $E\{ \nu^t \nu\}$ can be minimized by choice of $\underline{a}$ through solution of the linear equation

$$(\underline{X}^t \underline{X} + \Sigma)\underline{a} = \underline{X}^t y \qquad (2\text{-}14)$$

Equation 2-14 is just a simple modification of the standard regression equations ($\Sigma = 0$) and can easily be solved. Unfortunately, unlike the standard equations there appears at this time to be no method for solution that avoids the computation of $\underline{X}^t \underline{X}$. Therefore, care is needed to ensure accurate solutions.

2.3 SUMMARY

In this section we have discussed several issues that must be addressed in the development of an expanded-envelope residual generator. The adaptation mechanism we considered is a model scheduling mechanism as opposed to a model "learning" mechanism to avoid the problem of false adaptation to the failures we wish to detect. Effects that need to be considered include both large-amplitude maneuvers and changes due to Mach and altitude. The effect of large maneuvers at a single flight condition involves nonlinearities and interactions that are normally not considered in a linear aerodynamic model (e.g., for control design). Significant changes may also occur as a function of Mach and altitude because of the flexibility of the aircraft and the effect on load distributions due to flight condition. Qualitative prediction of the large maneuver effects is possible through physical arguments involving standard aerodynamic concepts. The so-called "static flexibility" effects are less understood and, therefore, require explicit scheduling using look-up tables.

For large maneuver effects, the scheduling is accomplished "implicitly" by construction of an analytic nonlinear model. This model is derived as a simplification to a mature aero package, although advanced identification techniques could be directly applied to flight test data

as well. The development of a useful nonlinear model for the residual generation process should incorporate physical understanding of aerodynamics (to avoid complex and/or overfitted models) and must consider the effects of sensor noise in determining the utility of individual elements of the model. Physical understanding led to a "panel method" model format. This format, however, had several drawbacks and led to the consideration of a quasi-linear model. This model assumes the form of a linear aerodynamic model, but with "derivatives" that are modeled as a function of other variables. The selection of which variables influence which "derivatives" is then justified from a physical standpoint. When the quasi-linear model is further expanded into a "parameter-linear" format, regression analysis can be used to estimate the best set of parameters. We then derived a modification to standard regression methods that explicitly deal with sensor errors in determining optimal residual generation parameters.

SECTION 3

DESIGN METHODS FOR EXPANDED ENVELOPE OPERATION DECISIONMAKING

In this section, we discuss the issues that must be addressed in the design of an expanded-envelope decisionmaking process for the FDI algorithm of [2] and develop methods that can be used in the design and evaluation process. As was the case with single flight condition designs, we concentrate on the problem of system robustness by adapting a decision structure based on design models of residual behavior and select parameters to optimize performance with respect to appropriate truth models.

For this work, we assume that the structure of the decision process has been determined and that we desire an adaptation mechanism for the parameters of this process. Furthermore, we shall assume that the temporal characteristics of the residuals do not change so that the filtering requirements for all statistical tests can be determined a priori. Thus, referring to the decision process described in [2], methods for scheduling the projections and thresholds of the various statistical tests within that process are sought.

3.1 DESIGN ISSUES

The decision mechanism developed in [2] utilizes knowledge about the unfailed and failed characteristics of the residuals in order to make accurate and timely failure decisions. "Adaptation" is required for full envelope operation because the statistical characteristics of the residuals (failed and unfailed) change over the flight envelope and because the design of a decision mechanism for "worst-case" scenarios is not adequate (either too low detection probabilities for acceptable false alarm rates, or too high false alarm rates for acceptable detection performance).

As in the design of decision mechanisms at a single flight condition, adaptation is based on knowledge about the statistical characteristics of the residuals (under both failed and unfailed operation). As in [2], we assert that a statistical characterization of the residuals under no-fail conditions is sufficient for evaluating failure detection performance. That is, let F denote a vector containing parameters whose changing values cause significant changes in the statistical characteristics of the residuals (it is not a trivial problem to determine what F consists of and/or provide measures of its components for use in adaptation; these issues are discussed at the end of this subsection). The six dimensional vector of residuals, ν, is modeled as (see [2], subsection 5.1.2);

$$H_0 \text{ (no failure)} \; : \; \nu(t) = n(t; F) \tag{3-1}$$

$$H_i \text{ (i-th failure)} : \; \nu(t) = n(t; F) + C_i(F)\, f_i(t) \tag{3-2}$$

The notation n(t; F) denotes a stochastic process that represents various kinds of errors (modeling, sensor, etc.) whose power spectral density (PSD) is a function of F. The notation is somewhat misleading since F changes as a function of time, thereby making the notion that the residual PSD is a function of F incorrect. However, if F changes slowly with respect to the FDI time scale this characterization is valid for design (this is not always the case; e.g., increases in low frequency error at high angular rates; thus caution must be used in interpretation of performance results).

In the design of the single flight condition decision mechanism, the statistical characteristics of the residual errors under no-failure conditions and the direction of the failures in residual space were mapped onto decisionmaking parameters using a well defined design methodology. Equations 3-1 and 3-2 imply that the first step in adaptive decisionmaking design is the characterization of the statistics of the unfailed residual errors n(t; F) and the characterization of the failure directions $C_i(F)/\| C_i(F) \|$ (defined as e(F) in the remainder of this section).

Several factors affect e(F) and the statistics of n(t; F). For example, situations that result in variations in the statistics of n(t; F) include :

1. The effect of sensor noise on the broadband energy content of the residuals is modulated by the size of the aerodynamic derivatives and the value of $\bar{q}$. This is because the residual model contains products of derivatives, $\bar{q}$ and sensor measurements. At higher $\bar{q}$, and for larger derivatives, the variance of the white noise portion of the residuals would be expected to increase.

2. Scale factor errors and sensor misalignments result in low-frequency or in-band errors. The size of this effect is also dependent on the size of appropriate derivatives and $\bar{q}$ with larger values implying larger residual variances. Misalignment errors are also a function of the size of maneuvers.

3. When model error is adequately characterized by an error (additive or multiplicative) in the derivative factor, then larger low-frequency errors are expected for large maneuvers. This includes maneuvers due to pilot commands, and large departures from steady flight due to disturbances (e.g., turbulence).

4. The residual model is based on static airflow and therefore errors during transients are expected. The errors are transient in nature, but could be considered low-frequency with respect to the FDI bandwidth.

Situations that result in variations in e(F) include, in principle, anything that can cause the control derivatives, C_i (F), to change. However, there are cases in which C_i(F) is not constant, but where the failure directions remain fixed. In these cases, adaptation is unnecessary. A two-dimensional example is given below.

Let a two-dimensional residual, under failed conditions (no uncertainty), be modeled by,

$$v_1 = c_1 g_1^f(d_f; F) - c_1 g_1^m(d_m; F) \qquad (3\text{-}2a)$$

$$v_2 = c_2 g_2^f(d_f; F) - c_2 g_2^m(d_m; F) \qquad (3\text{-}2b)$$

where d_f and d_m are the actual and measured control element values and g^f and g^m are actual (failed) and modeled control nonlinearities. The failure direction is defined by $\tan^{-1}(v_1/ v_2)$ and is a constant when

$$c_1 (g_1^f - g_1^m) / c_2 (g_2^f - g_2^m) = \text{constant} \qquad (3\text{-}3)$$

For example, $g_i^f = g_i^m = K_i(F) + g(d; F)$ satisfies Eq. 3-3. Thus, when control nonlinearities are the same in all axes, the failure directions remain constant and adaptation is not required.

A more problematic situation arises when the i-th failure direction changes as a function of the i-th control element deflection (i.e., one component of F is δ_i). Recall that the term adaptation in this project refers to a scheduling of design parameters as a function of measurable or estimable quantities. Now, if the failure directions can not be estimated or measured, adaptation is not possible. This is precisely the case when the i-th failure direction changes as a function of the i-th control element deflection. To see this, consider Eq. 3-2 again. Now, unless the functional form of the control derivative vectors satisfies Eq. 3-3, the left hand side of Eq. 3-3 (the failure direction) will be a function of the unmeasurable quantity d_f. If this effect is significant, and the performance obtained by assuming it is negligible is not adequate, then decision mechanism concepts that are radically different than those described so far may be required (e.g., more explicit failure-mode modeling, or the use of probe or dither signals for enhancing identifiability).

The extent of this situation was briefly investigated using the AFTI-F-16 model provided by NASA. Figures 3-1 through 3-6 are plots of the aerodynamic coefficients for NASA's F-16 model at h = 15,000 ft and M = 0.6 versus the deflection of a single control element (dfl, dhtl, and dr) with all other variables (other control elements, α, β, and angular rates) set to zero . These figures show that in all but a few cases, control effectiveness is linear for a substantial portion of the deflection range. The exceptions include C_x for all control elements (as one would expect from physical principles; i.e., drag > 0) and the pitching moment (C_m) due to flaperon deflection (dfl). Since, from past experience, C_x carries little information for detecting and isolating these control surfaces, there is little lost in eliminating C_x from consideration. Thus, the only problematic situation is the C_m vs. dfl nonlinearity. Figure 3-7 shows a plot of the C_m direction-cosine as a function of dfl for various values of dhtl. This plot shows that the failure direction for dfl changes with dfl deflection, and that this change interacts with dhtl deflection. Thus, we can not make use of the pitching moment

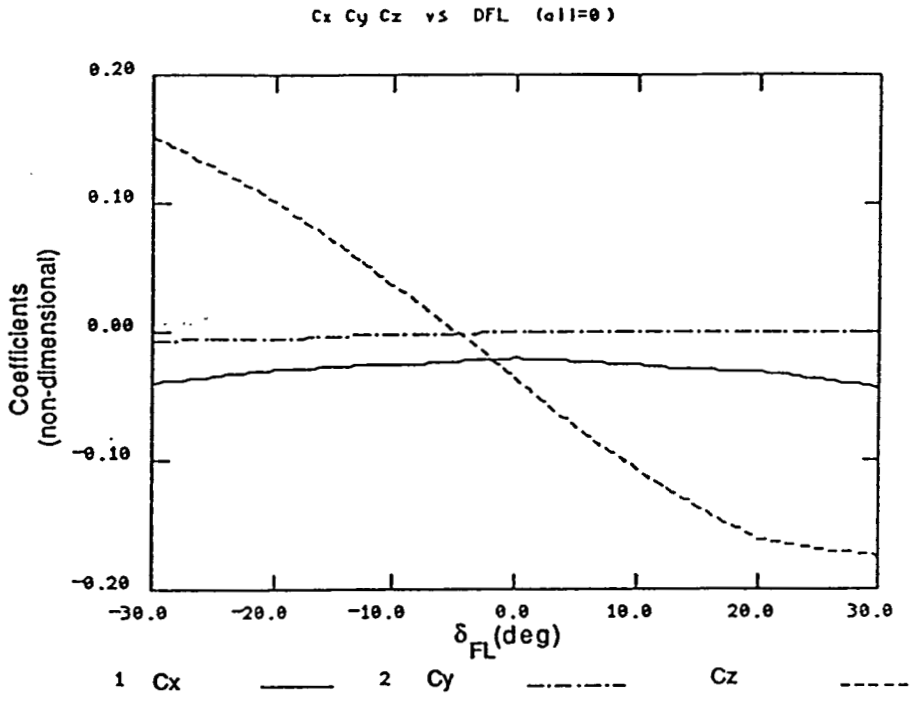

Figure 3-1. Cx Cy Cz vs. DFL (all=0).

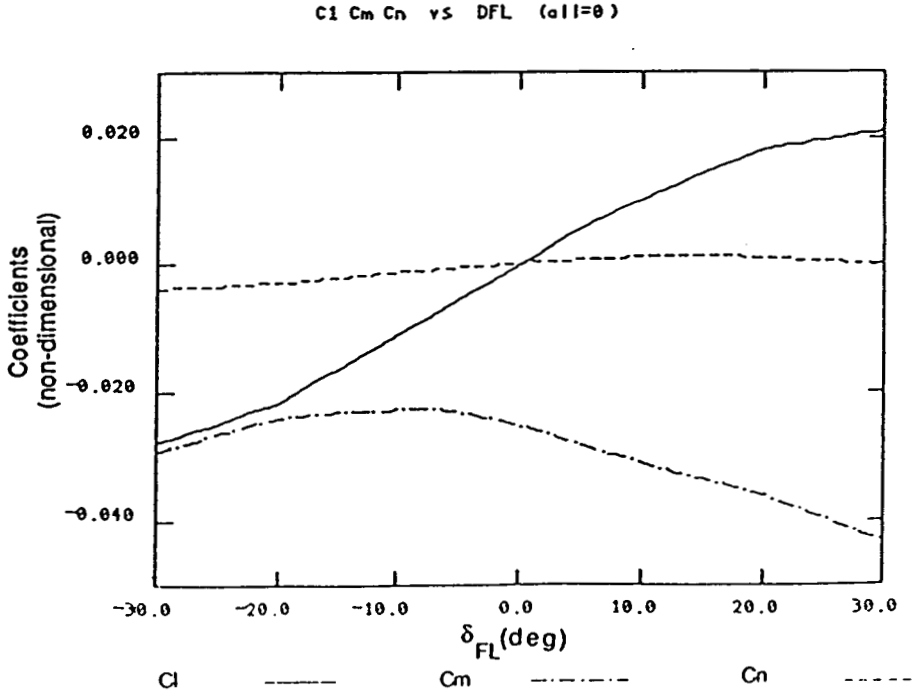

Figure 3-2. Cl Cm Cn vs. DFL (all=0).

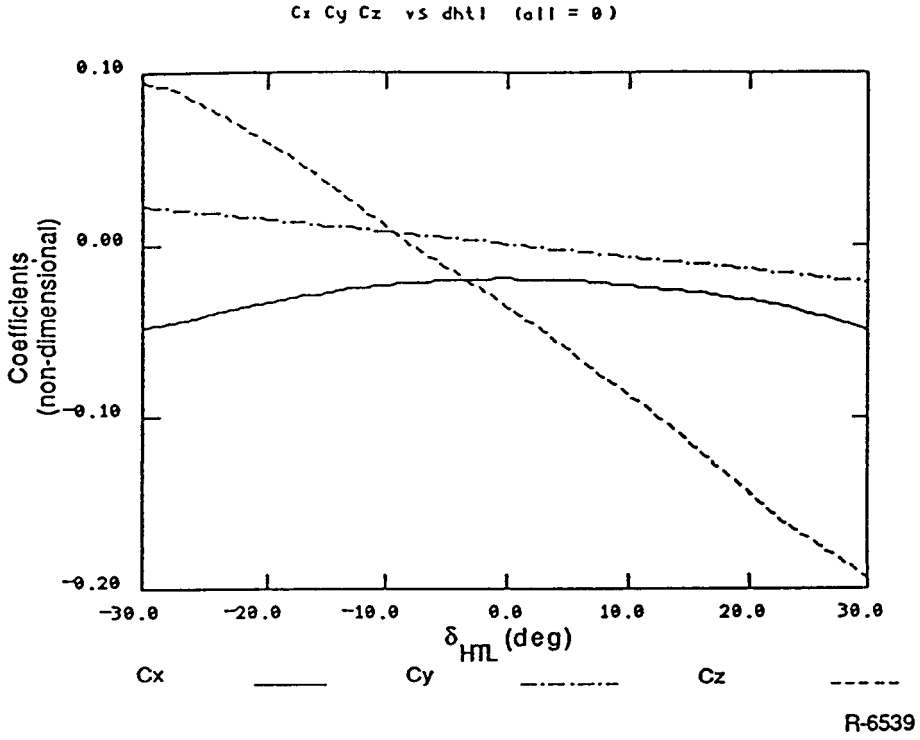

Figure 3-3. Cx Cy Cz vs. dhtl (all=0).

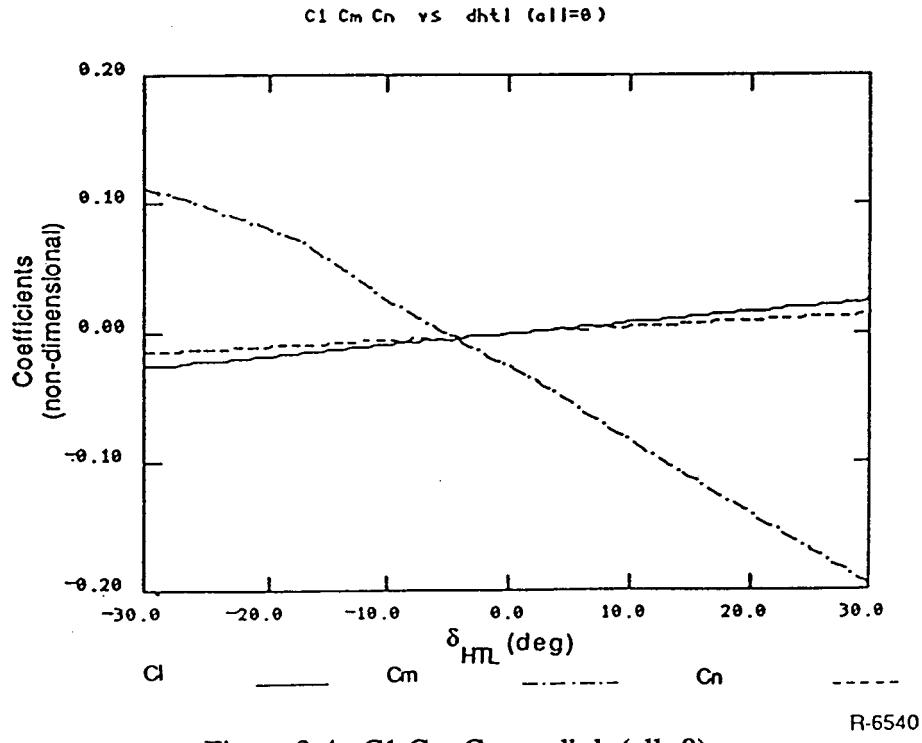

Figure 3-4. Cl Cm Cn vs. dhtl (all=0).

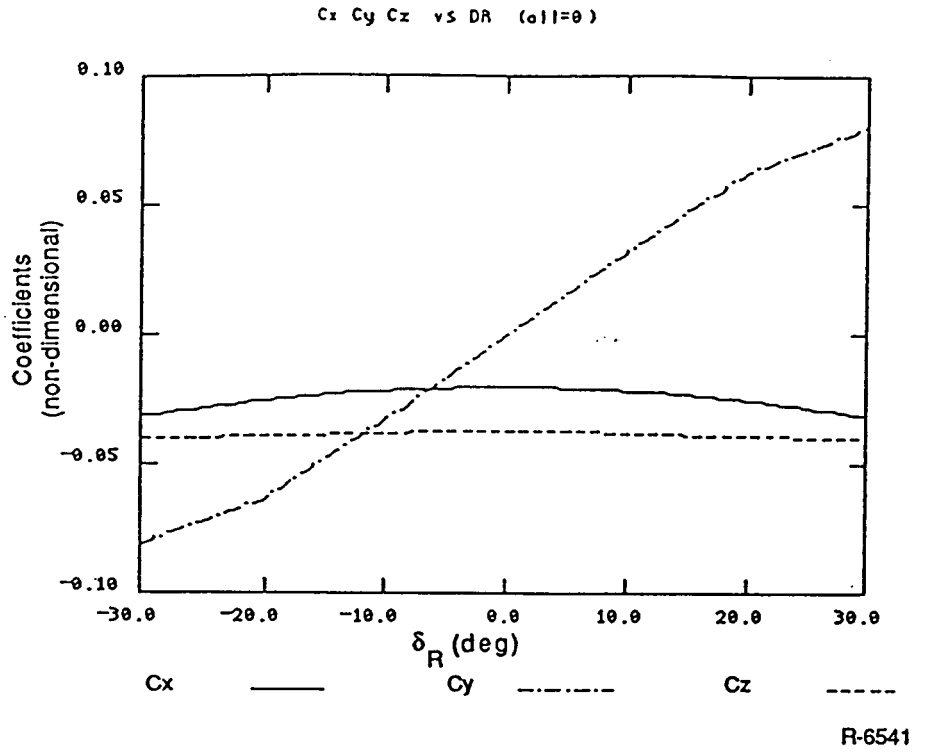

Figure 3-5. Cx Cy Cz vs. DR (all=0).

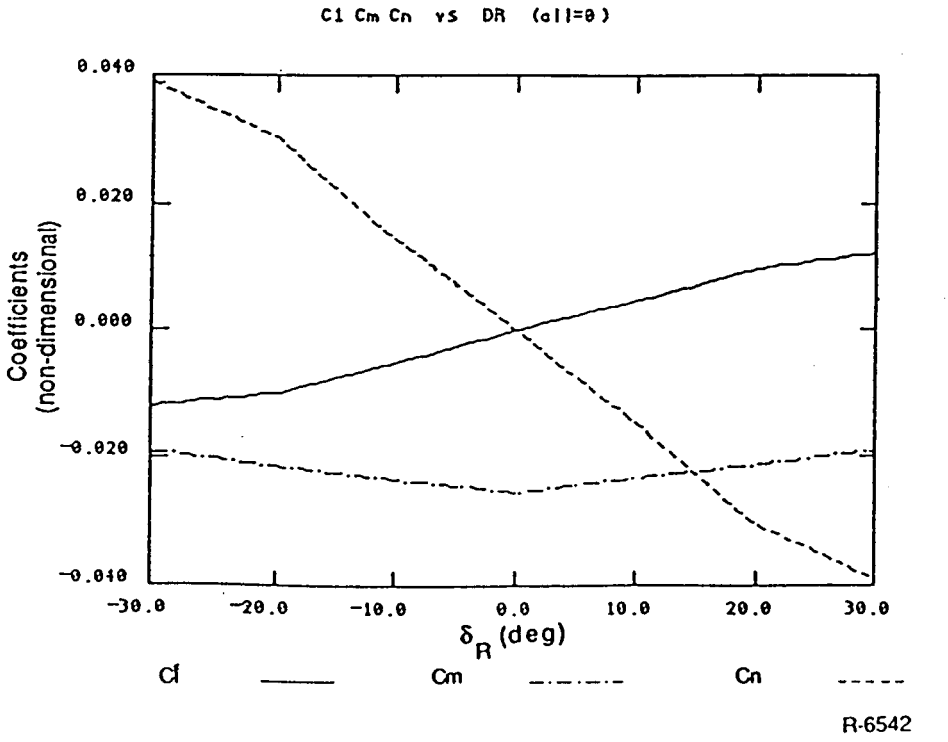

Figure 3-6. Cl Cm Cn vs. DR (all=0).

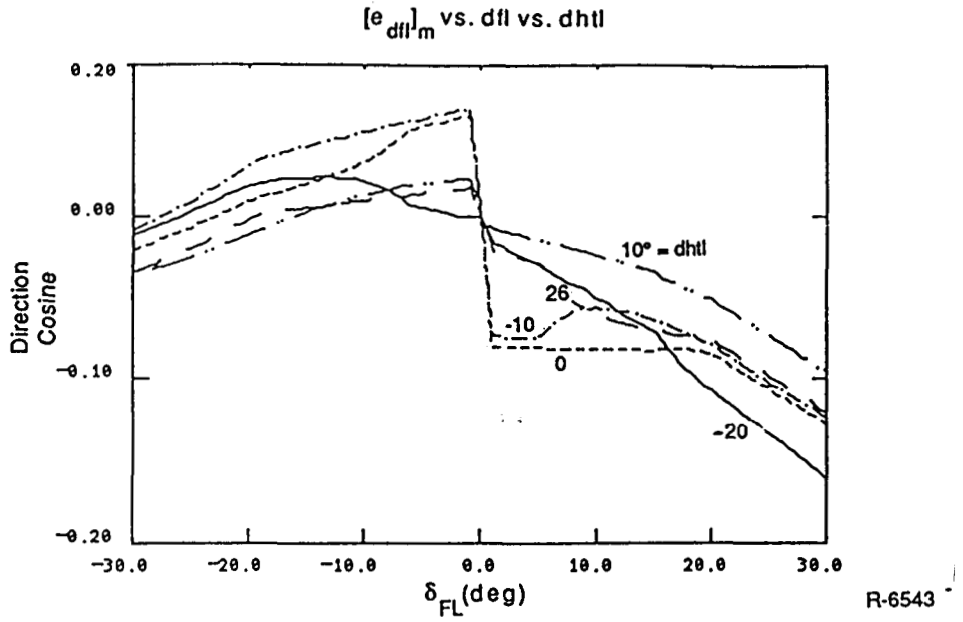

Figure 3-7. Pitch Moment Direction Cosine vs. dfl vs. dhtl.

residual for detecting or isolating dfl without further analysis of the impact of any simplifying assumptions that would need to be made (e.g., assuming C_m vs dfl is linear, or zero).

The above discussions have outlined some of the factors that might affect the statistical characteristics of n(t; F) and the failure directions e(F). The components of F should therefore be based on these factors either directly (e.g., by scheduling with $\bar{q}$, p, α, etc.) or indirectly. Although time did not permit a complete investigation of the appropriate composition of F for the AFTI-F-16, some general ideas can be developed. First, changes in the failure direction, e(F), can only occur as a function of those factors that also affect the corresponding control "derivatives" in a quasi-linear residual generation model. Therefore, the residual generation model provides a basis for identifying these factors. Plots of direction cosines vs. various factors can point to those factors that most influence failure directions and measurements of these factors may then be used to schedule those decisionmaking parameters that are affected by e(F). Secondly, some of the changes in the statistics of n(t; F), may also be derived by reference to the residual generation model. For example, dynamic pressure clearly has a direct influence on the size of the impact on additive sensor errors and should therefore be one factor upon which to schedule those decisionmaking parameters that are influenced by n(t; F)

characteristics. Similarly, significant changes in the size of the "derivatives" in a quasi-linear model may also influence the extent of the impact of additive sensor errors on residual errors. Some effects, however, are not easily characterized through reference to the residual generation model. Primarily, these are the effects that are modulated by the size of maneuvers (e.g., aero-model error, scale-factor error, misalignment error). One way to overcome the difficulty associated with characterization of these types of errors is through an empirical approach. In such an approach, a high fidelity simulation or data from a flight test vehicle would be processed to generate residuals (as we did in [2]). Flight condition elements (components of F) might include, in addition to the obvious factors such as $\bar{q}$, a specification of the size of the "inputs" (pilot inputs and wind disturbance) to the aircraft. Measures such as RMS stick deflection and RMS α-vane and β-vane movement (over an appropriate window) could then serve as "measurable" factors upon which scheduling may be based. Statistical characterizations of residual error can be computed from observations of the residuals and the parameters of such a characterization correlated with the RMS input measures.

Having characterized both e(F) and the statistics of n(t; F), we can then concentrate on the mapping from the statistics of n(t;F) and e(F) to the decisionmaking parameters. If a simple analytic mapping were available, the design process would now be complete (with the analytic calculations done on-line as a function of measured/estimated values of F). However, the mapping from the statistics of n(t;F) and e(F) to the decisionmaking parameters is sufficiently complex to require the consideration of methods of simplification that directly produce decision parameters as a function of F. Analytic methods for performing this part of the design process are considered in the next subsection.

3.2 DESIGN METHODS

In this subsection, we develop several methods for simplifying the relationships between a set of flight condition parameters, F, and the parameters of the decisionmaking process. In reference to the decision process of [2], the decisionmaking parameters that must

be specified include projection vectors and thresholds for the various hypothesis tests that must be performed. In principle, the filtering requirements for each test might also be specified; however, for this project, we have assumed that these requirements will not change over the flight envelope and therefore concentrate on threshold selection and projection vector design. In the following, a general design procedure is developed in which various design calculations are made. These calculations utilize many of the techniques discussed in [2] and will be referred to throughout this subsection. Methods for performing the relevant calculations are then provided for fixed sample size tests. Methods for designing sequential tests are the same for projection vector design; however, as discussed in [2], sequential test threshold design must use heuristic methods.

3.2.1 General Methodology

The main goal of this methodology is to develop a mapping from F to the decisionmaking parameters (thresholds and projection vectors) that is neither overly complex so as to require extensive amounts of computer time and/or memory nor too simple such that performance may be sacrificed. In general, threshold and projection vector selection are treated in a similar manner to the single flight condition design process. Having specified the filtering requirements of a particular test, selection of "optimal" (or near-optimal) projection vectors is performed. This selection process uses the n(t; F) and e(F) characterizations as the "truth-model" upon which performance is to be optimized. Having chosen the projection vectors, thresholds are then chosen to achieve acceptable decision-error characteristics.

The general design process attempts to strike a balance between the extremes of oversimplification and excessive complexity. At the simple end of this spectrum is a design that ignores all changes in n(t; F) and e(F) and employs a single set of (best) parameters. Should such a design achieve acceptable performance levels it is clearly the preferred solution. On the other end of the complexity spectrum is a design that specifies parameters at each of many values of F (i.e., many single flight condition designs) and performs interpolation of

these values when the actual F lies between the scheduling points. This method comes closest to optimal extended-envelope design, but will miss the fact that many of the schedules may be unnecessary. Thus, we seek a design method that can strike a balance between the simple "fixed-parameter" solution and the complex "variable-parameter" solution to come up with a partial "fixed/variable parameter" design. The key question to be answered in the development of a fixed/variable design is then "Which parameters can be fixed and which must vary to achieve adequate performance?"

Figure 3-8 shows an overview of the general design process. The process involves four basic steps progressing from the simplest design (fixed parameters) to the most reasonable tradeoff between performance and complexity in a partially fixed/variable design. Evaluations are made throughout the method to assess the impacts of simplifications in terms of performance reduction with respect to both the performance goals and the variable parameter design.

The first step in the process is to design and evaluate a fixed parameter system. Variations in e(F) and n(t; F) are taken into account in selecting a single best set of parameters for all values of F. Evaluations with respect to performance averaged over all values of F are made and compared to the design goals. If detection of important failures within reasonable amounts of time without too many false alarms can be achieved, then the fixed parameter system may be used and no scheduling is required. However, if the performance tradeoffs are unacceptable (e.g., thresholds set to avoid false alarms result in inadequate detection capability), continued development is needed.

The second step is the development of a completely variable design. In this step, a new set of parameters at every value of F (although F may be continuous valued, we assume continuity of its influence on n(t; F) and e(F) so that samples of F at appropriately spaced points will provide an adequate approximation to the continuous relationship between F and the design parameters) is computed . Evaluation of this design is made and used as a bound to performance levels achievable in any fixed/variable designs.

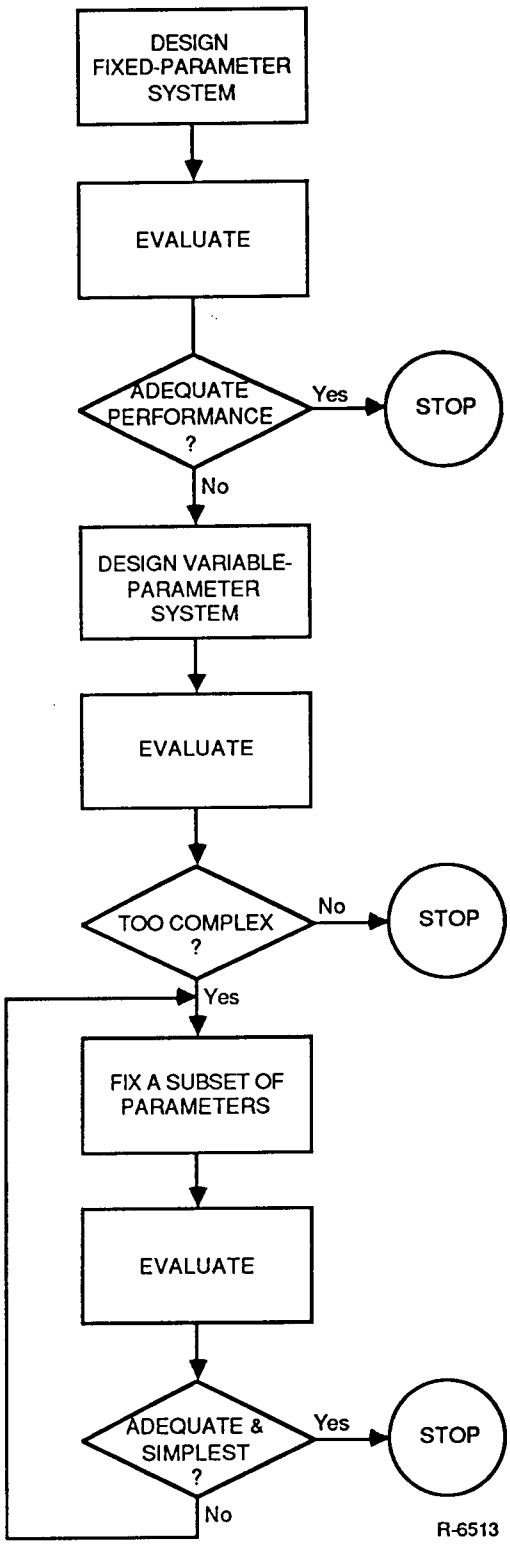

Figure 3-8. General Design Process.

The third step is taken if the variable design in step 2 is of sufficient complexity to warrant simplifications (note that no performance improvements over the step 2 design are possible with this procedure). In this step, the variations in the design parameters are examined and those variations that are deemed insignificant are selected as fixed parameters and a fixed/variable design is performed. The resulting design is evaluated and compared to the variable-parameter design and the design requirements to determine: a) if the design is acceptable (in terms of performance and simplicity), and b) if the selection of fixed parameters should be extended or another set chosen. The evaluation must occur because of the fact that what appear to be small variations in qualitative terms when selecting fixed parameters may actually represent important variations in terms of performance (this is due to the unequal scaling of the residuals).

The last step involves simplification of the relationship between F and those decision-making parameters that must vary as a function F to achieve adequate performance. This step is only necessitated if on-line data restrictions are such that storage of decisionmaking parameters at the various design points (F_k) (and subsequent interpolation between points) is not possible. As in the case of residual generation models, this last step involves model selection and regression analysis to fit a closed form approximation to the desired relationship. Note also that such a methodology can also be used to reduce the number of points in a look-up and interpolate model.

The general methodology has several computational requirements both for design and evaluation. In the next four subsections, details of these calculations are provided. First, methods of evaluation for any decisionmaking design are treated, and then methods for optimizing performance over the entire envelope are discussed.

3.2.2 Evaluation Methods

This section presents an evaluation method that can be used in the general design method discussed in the previous subsection. Many of the detailed calculations are similar to

those reported in [2] and proofs are therefore not provided in this report. Furthermore, we treat only fixed-sample size hypothesis tests (i.e., trigger tests). The design of sequential tests (verify and isolate tests) must follow ad-hoc procedures as in [2]; however, these procedures are typically based on fixed-sample size test designs so that the presentation below can be easily adapted. We also only deal with detection tests in the following (trigger and verify tests). Isolation tests can be treated in a similar manner as was done in [2].

For this development, we assume that the residual vector, under no-failure (H_0), at the k-th flight condition, F_k, is modeled by the residual error "noise" $n(t; F_k)$, while during failure of the i-th control element (H_i) at the k-th flight condition the residual can be modeled by

$$\nu = C_i(k) \cdot f \cdot + n(t; F_k) \tag{3-4}$$

(Note that Eq. 3-4 assumes a constant failure signature. Methods for dealing with other temporal characteristics are derived in [2], Section 4). The hypothesis tests that need to be designed and evaluated all take the form

$$\begin{aligned} &\text{Decide } H_i \text{ if } s(k) > t(k) \\ &\text{Decide } H_0 \text{ if } s(k) < t(k) \end{aligned} \tag{3-5}$$

where

$$s(k) = \left| P^t(k)\, \nu_f \right|$$

and

$$\nu_f = \text{filtered version of } \nu.$$

(We use the notation "x(k)" to indicate dependence of x on F_k).

Given the statistical characteristics of $n(t; F_k)$, the covariance matrix of ν_f, $\Sigma_f(k)$, can be derived. Thus, under no-failure, s is zero mean with variance given by

$$\sigma_0^2(k) = P^t(k)\, \Sigma_f(k)\, P(k) \tag{3-6}$$

Under H_i, the statistic, s, has a nonzero mean and variance given by

$$\bar{s}_i(k) = f\, P^t(k)\, C_i(k) \tag{3-7}$$

$$\sigma_i^2(k) = \sigma_0^2(k) = \sigma^2(k) \tag{3-8}$$

Now, the above equations give the (assumed Gaussian) probability density function for the statistic, s, at each flight condition. For evaluation, however, we need to summarize performance over all flight conditions. For this work, we propose to use average (over all flight conditions) values of relevant performance measures such as detection probability for a given failure signature, minimally detectable fault-signature for a given level of detection and false alarm probability. Alternate measures (to averages over all flight conditions) include the worst-case values or squared-mean-minus-variance values (for those measures that should be maximized) and mean square values (for those that should be minimized). For average values the relevant equations are;

Average "Signal-To-Noise"

$$d^2 = \sum_k \pi_k d^2(k) \tag{3-9}$$

where

$$d^2(k) = \frac{\left(P(k)^T C_i(k)\right)^2}{\sigma^2(k)} f^2$$

Average Minimal-Detectable Failure

$$f_{min} = \sum_k \pi_k f_{min}(k) \tag{3-10}$$

where

$$\frac{\left(f_{min}(k)\ \left|P(k)^t C(k)\right| - t(k)\right)}{\sigma^2(k)} = Q^{-1}(P_d)$$

and,

Average Probability of False Alarm

$$P_{fa} = \sum_k \pi_k Q\left(\frac{t(k)}{\sigma^2(k)}\right) \tag{3-11}$$

In the above, π_k represents a weight associated with the k-th flight condition, $Q^{-1}(\xi)$ is the inverse of the Gaussian error function, and P_d is the desired detection probability. Note that Eq. 3-9 does not include evaluation of the selected t(k) since it presumes that t(k) is selected to realize a tradeoff between false alarms and missed detections that is specified by $d^2(k)$.

3.2.3 Variable Design Method

The simplest design procedure is that used in the variable design. This method is tantamount to several single flight condition designs; one for each value of F_k. Thus the methods discussed in [2] are used at each F_k. The relevant equations are:

$$P(k) = \frac{\Sigma_f^{-1}(k)\, C_i(k)}{\| C_i(k) \|} \tag{3-12}$$

$$t(k) = \sigma^2(k)\, Q^{-1}\,(P_{fa\ desired}) \tag{3-13}$$

These values can then be used in Eq. 3-9 or 3-10 to evaluate the design.

3.2.4 Fixed Parameter Design Method

The next simplest design procedure is the fixed-parameter system. This method tries to select a single optimal set of values for all flight conditions. Thus, P(k) = P and t(k) = t for all k. To choose P, we would like to optimize d^2 (as in [2]) as given by Eq. 3-9. Rewriting Eq. 3-9 to highlight full the dependence on P we have

$$d^2 = \sum_k \pi_k \frac{P^T\left[C_i(k)\ C_i(k)^T\right]P}{P^T\left[\Sigma_f(k)\right]\ P} f^2 \tag{3-14}$$

Unfortunately, unless $\Sigma_f(k)$ is a constant, the optimal solution of Eq. 3-14 for P is not closed-form, [9]. Thus an alternate performance measure is desired. One way to solve this problem is to use a modification to Eq. 3-14 that represents the ratio of average mean of s (over all flight conditions) to average variance of s, namely,

$$\frac{P^T R_c P}{P^T \overline{\Sigma}_f P} \tag{3-15}$$

where

$$R_c = \sum_k \pi_k C_i(k)\ C_i(k)^T \tag{3-16}$$

$$\overline{\Sigma}_f = \sum_k \pi_k \Sigma_f(k) \tag{3-17}$$

It is easy to show that this measure is maximized by

$$P = \overline{\Sigma}_f^{-\frac{1}{2}} V \tag{3-18}$$

where V is the eigenvector corresponding to the smallest eigenvalue of the matrix

$$\left[\overline{\Sigma}_f^{-\frac{1}{2}} R_c\, \overline{\Sigma}_f^{-\frac{1}{2}}\right]$$

Another way to solve the problem is to treat F as a random variable taking on values F_k with probability π_k. Then, approximate Gaussians are used to model the weighted sum of Gaussians densities that characterizes s over the entire flight envelope, for each hypothesis (failed and unfailed). Even if the Gaussian densities with the same mean and variance are used, the result is another optimization problem that has no closed form solution. Therefore, this method is not considered further.

Now, to select the single best threshold, we try to achieve low false alarms at all flight conditions. Thus choosing t to minimize Eq. 3-11 would be desired. Unfortunately, the

solution can not be expressed in closed form (even if standard approximations are made to the error function) and is, therefore, deemed inappropriate for this effort. If we use the average variance to characterize the variations under all flight conditions, however, a reasonable selection of t can be made from

$$Q\left(\frac{t}{\sum_k \sigma^2(k)\,\pi_k}\right) = P_{\text{fa desired}} \quad . \tag{3-19}$$

3.2.5 Fixed Plus Variable Design Method

In this design stage, we wish to fix some of the parameters of the decisionmaking process as a function of flight condition, F_k, and allow others to vary. Such a design allows compromises between performance and complexity to be made. For this development we will refer to P_f and $P_v(k)$ as the fixed and variable parts of the projection vector, P(k), respectively and similarly for t_f and $t_v(k)$.

Threshold setting requires definition of P(k) and is straightforward. For those F_k that require different thresholds, Eq. 3-13 is used. Those F_k for which a single threshold is desired can be treated using Eq. 3-19, where the sum over k represents only those flight conditions for which a single threshold is desired. Deciding which flight conditions need a separate threshold, and which can be grouped together with a single flight condition is not treated in any detail in this report. However, we observe that a single threshold will be sufficient for all those values of F (and P(k)) that result in variances for s that are nearly equal.

Choosing fixed and variable portions of P requires, as in the fixed design method, a measure of overall performance that is both relevant and functionally related to P_v and P_f in such a way that either closed form solutions or straightforward optimization procedures can be used (although elaborate solution methods may be available, it is not deemed of sufficient importance to the overall design problem to warrant the attendant development effort). To

illustrate the idea of fixed plus variable design, consider a case in which $\Sigma_f(k)$ is constant and equal to the identity matrix. In this case we have,

$$d^2(k) = \left[P_v(k)^T C_i^v(k) + P_f^T C_i^f(k) \right]^2 . \qquad (3\text{-}20)$$

To maximize $d^2 = \Sigma \pi_k d^2(K)$ requires that we first maximize each d(k) resulting in optimal values of $P_v(k)$ as a function P_f. Then we can solve for the optimal P_f, (this is because the $P_v(k)$'s affect only d(k)). In a three residual system, for example, d(k) is

$$d(k)^2 = \left[P_1 [C]_1 + P_2 [C]_2 + P_3 [C]_3 \right]^2 \qquad (3\text{-}21)$$

In Eq. 3-21, the notation $[C]_i$ denotes the i-th element of the vector $C_i(k)$ and the dependence of the elements of the $[C]_i$ on F_k has been suppressed, and P_i is the i-th element of P(k). Now suppose we allow P_1 and P_2 to vary with k and require P_3 to be constant. Then maximizing Eq. 3-21 by choice of P_1 and P_2 (with the usual $\| P \| = 1$ restriction) gives,

$$P_1 = \frac{[C]_1}{\left([C]_1^2 + [C]_2^2 \right)^{\frac{1}{2}}} \left(1 - P_3^2 \right)^{\frac{1}{2}} \qquad (3\text{-}22a)$$

$$P_2 = \frac{[C]_2}{\left([C]_1^2 + [C]_2^2 \right)^{\frac{1}{2}}} \left(1 - P_3^2 \right)^{\frac{1}{2}} \qquad (3\text{-}225b)$$

(We only need to maximize $P_v^T C_i^v$ since $d^2(k)$ is monotonic in this term). Substituting into Eq. 3-21 gives,

$$d^2(k) = \left[\left(1 - P_3^2 \right)^{\frac{1}{2}} \left(C_1^2 + C_2^2 \right)^{\frac{1}{2}} + P_3 C_3 \right]^2 \qquad (3\text{-}23)$$

Taking the average over all flight conditions gives an equation for P_3 of the form

$$d^2 = A_1\left(1-P_3^2\right) + A_2 P_3\left(1-P_3^2\right)^{\frac{1}{2}} + A_3 P_3^2 \qquad (3\text{-}24)$$

To maximize Eq. 3-24 the relevant gradient equation is

$$-2A_1 P_3 - A_2 P_3^2\left(1-P_3^2\right)^{-\frac{1}{2}} + A_2\left(1-P_3^2\right)^{\frac{1}{2}} + 2A_3 P_3 = 0 \qquad (3\text{-}25)$$

This equation is a transcendental one in P_3 and can be solved by standard iterative methods (e.g., Newton's method).

Now, when $\Sigma_f(k)$ is not the identity at all flight conditions, the situation is substantially more complex. Closed forms for this general case were not derived for this project, and so an ad-hoc procedure is now proposed. Suppose that instead of choosing the optimal value of P_f we select P_f to be some specific value (e.g., zero or the average over all values in a variable-parameter design). Given this selection we would like to optimize Eq. 3-9 through choice of $P_v(k)$. However, a closed form solution to this problem is not immediately obvious. Therefore, we choose $P_v(k)$ to optimze a d^2 metric in the reduced subspace of residuals corresponding to the variable elements of P. If we let $\Sigma_f^v(k)$ be the covariance of the filtered residuals in this subspace, then the solution is

$$P_v(k) \sim \Sigma_f^v(k)^{-1} C_i^v(k) \qquad (3\text{-}27)$$

and the result is normalized so that P has unit norm.

3.3 SUMMARY

In this section we have discussed various issues in the development of an adaptive decision mechanism (DM) for control element FDI. We assumed that the structure of the decision process was predetermined and that only the parameters of this process are to be "adapted." As in Section 2, the adaptation mechanism is a "scheduling" concept in which the decisionmaking parameters are changed as a function of "on-line" measurable flight-condition quantities. We also assumed that the temporal characteristics (i.e., spectral shape) of the

residuals are constant so that filtering requirements for each hypothesis test do not need to be scheduled.

Scheduling of DM parameters is potentially required whenever changes to the covariance of the filtered residuals occur and whenever changes to the failure directions occur. The former requires changes to both thresholds and projection vectors while the latter only requires changes to projection vectors. Although failure directions may change whenever the control derivatives change, if these changes effect all derivatives in a similar manner, then the failure directions remain constant. When all derivatives are not affected in a similar manner, scheduling of the projection vectors must occur. However, this is only possible if the parameters affecting the failure directions are measurable. Such is not the case when a failure direction is affected by its corresponding control element value. Should this occur (as it does for the flaperons on the F-16), care must be taken in the design of tests for flaperon failures (particularly in using the pitching-moment residual).

The measurable quantities upon which scheduling must be based include dynamic pressure, roll rate, and angle of attack, since their values has a direct impact on the sensor noise component of the residuals. However, other effects, such as those that are modulated by maneuver size are more difficult to describe. One way to establish scheduling requirements for these effects is to perform an empirical study (using either a high-fidelity simulation or flight-tests) and to schedule parameters as a function of the "size" of aircraft "inputs."

Once the flight-condition parameters are defined, the DM design goal becomes one of balancing complexity and performance of the scheduling mechanism. The simplest DM design is a fixed-parameter solution and should be used if its performance is adequate. At the other extreme is a DM design in which all parameters must be scheduled. In between these extremes a partial fixed/variable design allows for some parameters to be fixed and some to vary as a function of flight condition. Design and evaluation methods were given for all three DM design concepts.

SECTION 4

RESIDUAL GENERATION FOR THE AFTI/F-16

4.0 INTRODUCTION

A key component to developing an aircraft-path FDI algorithm for expanded envelopes of operation is a residual generation process that is adaptable over a large range of flight conditions. Such a residual generation process must provide accurate estimates of the aircraft during normal flight and also during large scale maneuvers over a wide range of velocities and altitudes. To achieve a high level of accuracy in the prediction of the aircraft behavior, it is imperative that a high fidelity model of the aircraft be synthesized.

The purpose of this section is to build an expanded envelope, nonlinear residual generator and demonstrate its improvement over the single flight condition, linear residual generator. This process will be demonstated for a NASA AFTI/F-16. The general design methods and selected approach to the residual generation process were described in Section 2. The general method that will be used includes modeling the aircraft at various fixed flight conditions, but over a broad range of motions. Several models, developed in this manner but at different flight conditions, will be scheduled to account for the full operating range of the aircraft. (For this demonstration, however, only one model at a single flight condition was developed.) The selected approach for developing high fidelity models utilizes a nonlinear/ quasi-linear model (basically a polynomial of nonlinear functions, each of which can be reduced to a summation of "coefficents" times "predictors") and a regression analysis based on that model, as detailed in subsections 2.2.2 and 2.2.3.

Due to the limitations in scope of this project, several assumptions and simplifications were made. One of these simplifications, as mentioned above, is the development of only one nonlinear/quasi-linear model instead of the many that are required for full adaptability of the

residual generator. It was also decided to model only the roll moment axis, with the assumption that any results obtained could be similarly extended to any of the aircraft's other five degrees of motion. Other assumptions were made to reduce the complexity of the modeling process, such as simplifications to the sensor noise model, limitations placed on control deflections, etc., which are all explained in more detail in the sections below.

Despite these simplifications to the residual generation design, promising results were obtained from the test runs. It was clearly shown that a quasi-linear approach in formulating a nonlinear model resulted in much more accurate residuals than the standard linear model. In addition, the sensor noise computation method proved to be a workable concept despite low enough sensor noise levels that warranted exclusion of the actual use of the concept. The regression analysis showed that further reduction of the number of terms may be plausible, given that effectively no accuracy was lost in the reduction from 31 predictor terms to 22 predictor terms. Finally, avenues exist for further refinement through actual implementation of multiple flight condition models (which was not realized due to time constraints) and modeling of predictor terms as piecewise-linear models.

4.1 MODEL DEVELOPMENT

One of the primary goals in the development of the residual generation process is to determine the terms for inclusion in the quasi-linear equations of motion, or more specifically, the equation for the coefficient of rolling moment. These terms, if chosen judiciously, will provide a far better representation of aircraft behavior in multiple-flight condition sorties than the standard linear model. Until now, there had been no set method for choosing these terms. The method that is presented here for choosing the terms is based on the nonlinear/quasi-linear model detailed in subsection 2.2.2. Subsection 4.1.1 presents the approach that was taken to select the terms, including a description of the quasi-linear model and an outline of the steps in the prescribed method. Subsection 4.1.2 discusses the application to an F-16 of the method developed in the previous section, covering the selection of the potential predictor terms, and

presents the final terms that were chosen for the residual generation models. For such a method to be developed, many auxiliary issues also must be addressed. These include the development of a sensor noise model and computational isssues, such as sampling. These two topics are discussed in subsections 4.1.3 and 4.1.4.

4.1.1 The Approach

The method used to develop an accurate model of the aircraft incorporates aspects of the nonlinear/quasi-linear model as described in subsection 2.2.2, thus, a good understanding of the implementation of this model is necessary. A brief overview is provided here.

The quasi-linear model represents an aerodynamic, non-dimensional coefficient (in this specific case, the rolling moment coefficient, C_l) as a summation of nonlinear functions multiplied by a corresponding independent variable, namely,

$$C_l = \sum_i C_{l\,\psi_i} \psi_i \tag{4-1}$$

where ψ_i are the measurable quantities that are likely to affect C_l and each $C_{l\psi_i}$ is a nonlinear function, the derivative of C_l with respect to ψ_i. The above equation is a more specific version of Eq. 2-6. This polynomial can be simplified further if each term of the polynomial is expanded into a summation of coefficients multiplied by a reduced term (a predictor) such that,

$$\begin{aligned} C_{l\,\psi_i} \cdot \psi_i &= f_{\psi_i}(x_1, x_2, x_3 \ldots) \cdot \psi_i \\ &= g_1(x_1) \cdot \psi_i + g_2(x_2) \cdot \psi_i + g_3(x_3) \cdot \psi_i \ \ldots \end{aligned} \tag{4-2}$$

where x_1,x_2, x_3, etc., are arbitrary classes of "causal" variables of the nonlinear function, f; ψ_i are the measurable quantities mentioned above; and $g_j(x_j)$ is an n-th order polynomial in x (n to be determined later), that is, the contribution of the derivative , $C_{l\psi_i}$, due to x_j. The order of the polynomial $g(x_i)$ is determined by x_i's influence on the corresponding derivative.

A high order polynomial implies that all lower order variables are also required. Thus, the quasi-linear model can be concisely summarized as a polynomial,

$$C_l = \sum a_i x_i^n \psi_i \qquad (4\text{-}3)$$

where x_i^n is an n-th ordered variable, called the "causal" variable, such that if x_i^n exists, then all lower order variables of x_i also exist, and a_i is the "regression coefficient".

Clearly, given the arbitrary nature of x_i, it would be extremely difficult to try all combinations of possible independent variables of indeterminable order with each derivative. Thus a method was required to select the candidate nonlinear terms, that is, the nonlinear derivatives. From these candidate terms, the proper predictors (defined as the combination of $x_i\psi_i$) and their complementary coefficients can be deduced.

The choice of the quasi-linear candidate terms was accomplished by a deliberate approach that also required intuitive reasoning. This approach requires intuitive reasoning to create an original list of potential terms, which are selected based on aircraft dynamic properties and studies of sensitivity plots. These terms are reduced to potential predictor terms. A backward elimination regression analysis is then used to eliminate these potential predictor terms in the model one at a time. This elimination process is based on a figure of merit (FOM) of the predicted residual error variance.

The following steps outline the method that was developed to characterize the behavior of the AFTI/F-16:

1. **Select causal variables** - A general form of the aircraft equations of motion is taken as a starting point. Using the quasi-linear model approach, one variant of the aircraft equation of motion is an unrestrictive equation, such as equation (4-1) above. As noted in the equations describing the quasi-linear model (equations 4-1 to 4-3), the "predictor" is defined as consisting of two independent variables, ψ and x. In equation 4-2, the variable ψ is combined into the derivative $C_{l\psi}$, which is a function of many independent variables x. These x variables are called "causal" variables, that is, they cause the derivatives, $C_{l\psi}$, to vary. Although both the

causal variable and the independent variable, ψ, are predictor-type variables (and thus, a case could be made to form the derivative C_{l_x} instead of C_{l_ψ}), a causal variable is differentiated from ψ in that the causal variable is a variable that is not traditionally associated with predicting the dependent variable in question, i.e., the non-dimensional coefficient, C_l. The independent variable will always be the more influential of the two, the one commonly associated with the dependent variable. For example, if C_{l_β} is a function of α, then α would be referred to as the causal variable, β would be referred to as the independent variable, ψ, (since C_{l_β} is a common derivative whereas C_{l_α} is much less common) and C_l would be referred to as the dependent value.

The candidate nonlinear terms are drawn from physical explanations of the aircraft behavior. For each candidate term, a reasonable and workable list of causal variables are selected. This can be based solely on dynamic or static characteristics of the aircraft, or it may be empirically gathered from flight data. From this reduced set of nonlinear functions, simplifications can be made to the polynomial, as in equation (4-2), to arrive at the set of potential "predictors", or more accurately, "the class of predictors" (since for each class of predictors, $x_i^n \psi_i^n$, many combinations of predictors may exist). Each potential predictor's composition varies from linear terms (where no causal variable exists), to cross terms (where the causal variable is different from the independent variable, ψ), to single variable, higher order terms (where the causal variable is the same as the independent variable,ψ). The terminology used in the quasi-linear model development is summarized in the partial example below:

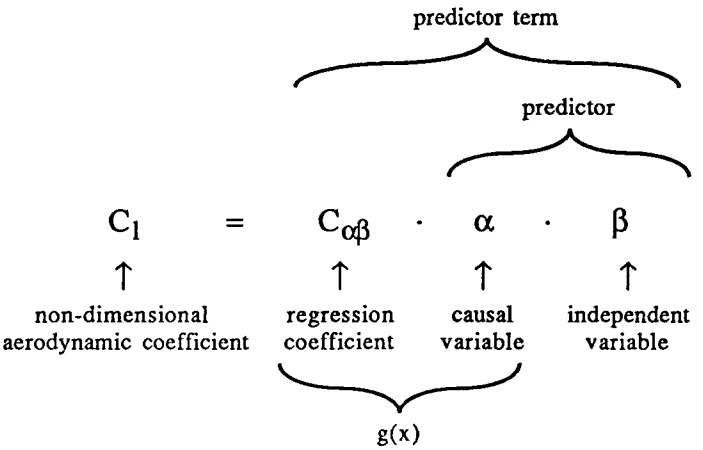

2. **Plot derivative sensitivities to causal variables** - For each suspected class of predictors, a plot of variations in the derivative over different values of the causal variables is made. For example, if collective flap deflections are suspected of affecting the coefficient of rolling moment due to β, then plots would be made of the coefficient of rolling moment due to β at several collective flap deflections.

3. **Determine predictor terms** - Each plot is analyzed to determine if the suspected causal variable actually changes the derivative value in question. If the plot shows a constant derivative value for all causal values, then the suspected class of predictors is removed from consideration. If, however, the plot varies, then the highest ordered effect of the causal variable must be determined through inspection of the plot. It is assumed that for a predictor whose causal variable was assigned order n, that predictors with causal variables of less than n will naturally exist.

From analysis of the plots, a list can be generated to separate all suspected terms into either large effects, small effects, or no effect.

4. **Perform backward elimination regression analysis** - With the predictors deduced from the above steps, a backward elimination regression analysis is implemented. Briefly, the backward elimination starts out by attempting to fit all predictors to the dependent values. After each regression step, the least influential predictor term is removed and the regression is repeated. This will continue until a manageable number of terms remain. One criterion used for deciding the number of terms to keep is the requirement that the sample variance of the nonlinear model have significantly better results than the linear model.

4.1.2 Application to F-16 Rolling Moment Model

This section describes the actual procedure used in developing the AFTI/F-16 nonlinear model. Since we will only concentrate on the rolling moment for demonstrating the effectiveness of an extended envelope residual generator, only the L-axis predictor terms are

eventually derived. The step numbers listed below correspond to the steps itemized in the previous section.

Step 1 - Select causal variables

The first step to creating a nonlinear model for the F-16 is to take a general form of the non-dimensional rolling moment coefficient and select from this equation the set of possible candidate nonlinear terms. Preferably, most of the candidate terms chosen will be deduced either directly from intrinsic qualities of the aircraft or from sets of terms used in other studies. For this specific task, terms were drawn from both sources.

An initial list of candidate terms was first compiled based on the theories of aircraft dynamics and control as detailed in Roskam [6] and McRuer [10]. From these sources, the rolling moment aerodynamic coefficient can be summarized in quasi-linear form as:

$$\begin{aligned} Cl &= \frac{b}{2V_T}\left(Cl_p(\alpha)\cdot p + Cl_r(\alpha)\cdot r\right) + Cl_\beta(\alpha, \delta_{FC}, \delta_{sp}, \beta)\cdot\beta \\ &+ Cl_{\delta_{FA}}(\alpha, \delta_{FC}, \delta_{FA})\cdot\delta_{FA} + Cl_{\delta_{HTA}}(\alpha, \delta_{FC}, \delta_{FA})\cdot\delta_{HTA} \\ &+ Cl_{\delta_r}(\alpha, \delta_{FC}, \delta_r)\cdot\delta_r + Cl_{\delta_{VC}}(\alpha, \beta, \delta_{VC})\cdot\delta_{VC} \end{aligned} \qquad (4\text{-}5)$$

The following gives a short explanation for the various causal variables of the nonlinear terms of the equation. The angle of attack affects all the derivatives because of its influence on the effective lift of the wings, which grows with increasing alpha below separation. The collective flap deflection is a factor in many of the derivatives due to its contribution to the altering of the effective camber of the wing. The tail derivatives are additionally affected by downwash caused by the flap deflections. The β derivative is also affected by the canard deflection, which adds an asymmetrical side wind component due to its location.

Each nonlinear derivative was then reduced to two-variable cross term predictors with indeterminable order. For example,

$$C_{l_\beta}(\alpha, \delta_{FC}, \delta_{sp}, \beta) = C_{l_\beta}(\alpha) + C_{l_\beta}(\delta_{FC}) + C_{l_\beta}(\delta_{sp}) + C_{l_\beta}(\beta) \qquad (4\text{-}6)$$

Of course, interactions involving more than two variables exist physically, but, as the results later will show, very accurate modeling can be attained by using only two variable cross-term predictors. This assumption, in effect, simplifies the model and limits the amount of coupling between variables to two at a time. The full list of the resulting Aero- "Derivatives" are shown in Table 4-1.

TABLE 4-1. AERO-MODEL "DERIVATIVES"

$C_{l_r}(\alpha)$	
$C_{l_p}(\alpha)$	
$C_{l_\beta}(\alpha, \delta_{FC}, \delta_{sp}, \beta)$	$= C_{l_\beta}(\alpha) + C_{l_\beta}(\delta_{FC}) + C_{l_\beta}(\delta_{sp}) + C_{l_\beta}(\beta)$
$C_{l_{\delta_{FA}}}(\alpha, \delta_{FC}, \delta_{FA})$	$= C_{l_{\delta_{FA}}}(\alpha) + C_{l_{\delta_{FA}}}(\delta_{FC}) + C_{l_{\delta_{FA}}}(\delta_{FA})$
$C_{l_{\delta_{HTA}}}(\alpha, \delta_{FC}, \delta_{FA})$	$= C_{l_{\delta_{HTA}}}(\alpha) + C_{l_{\delta_{HTA}}}(\delta_{FC}) + C_{l_{\delta_{HTA}}}(\delta_{FA})$
$C_{l_{\delta_r}}(\alpha, \delta_{FC}, \delta_r)$	$= C_{l_{\delta_r}}(\alpha) + C_{l_{\delta_r}}(\delta_{FC}) + C_{l_{\delta_r}}(\delta_r)$
$C_{l_{\delta_{VC}}}(\alpha, \beta, \delta_{VC})$	$= C_{l_{\delta_{VC}}}(\alpha) + C_{l_{\delta_{VC}}}(\beta) + C_{l_{\delta_{VC}}}(\delta_{VC})$

Step 2 - Plot derivative sensitivities to causal variables

A software package supplied by NASA Langley was used to generate data for plots of the effects of a suspected causal variable to a derivative. This software package produced aerodynamic coefficients modeled through look-up tables of the F-16. Since the output of the aerodynamics package gave the non-dimensional rolling moment coefficient and not the desired derivatives, each plot was actually a multiple plot graphic representing variations of two independent variables, the derivative-related, independent variable,ψ, and the suspected causal variable. For example, for a coefficient of rolling moment due to β, $C_{l\beta}$, (i.e., the variation of the dependent variable with respect to the independent variable) that is suspected to vary with α (i.e., the causal variable), the independent variable, β, would be plotted along the x-axis, but

there would be multiple plots of the rolling moment coefficient, one for each selected value of α. The independent variable, that is, β, was varied over the maximum range of possible values, e.g., -5 degrees to 5 degrees, while the suspected causal variable, that is, α, was set at five typical values (based on the flight tables generated from the simulation by NASA, e.g., -10, 0, 10, 20, 30 degrees). The plots of all suspected predictors that were examined are given in Appendix A.

Step 3 - Determine Predictors

From the plots created in step 3, the following generalizations and decisions were made in forming the nonlinear model. First, if a predictor with a relationship containing a high ordered variable appeared to exist , e.g., coefficient of rolling moment due to beta is related to alpha by alpha cubed, then all lower ordered predictors of the same relationship were also included for the regression analysis. Second, from observations of the plots, certain ranges of the plots exhibited nonlinear behavior. One example of this was in the plots of beta versus collective flaps (see Plot 3 of Appendix A), where the coefficient resembled a sum of two different plots. To actually attempt to characterize this plot as a polynomial would have required too many high order terms. Although modeling with high order terms may produce a better fit, it may also over fit the model thereby masking the actual intrinsic behavior of the system. One alternative to a polynomial solution is to use a piecewise linear approach. A simpler solution, however, is to limit the flight envelope for beta to plus or minus 2.5 degrees, which also limits the number of predictor terms needed in the model. Within this region, the characteristics are straightforward enough to require using only the first and second-order terms without need of a more complicated piecewise linear scheme. Although this may seem too restrictive, this limit did not restrict the effectiveness of the nonlinear model, as will be shown later in subsection 4.2.3. Similar reasoning led to constraints placed on the rudder deflection and the asymmetrical canard deflection. The limits to these three parameters are summarized below:

1. -2.5 < beta < 2.5 degrees

2. -20.0 < rudder < 20.0 degrees

3. -15.0 < asymmetrical canard < 15.0 degrees

Examination of the plots reduced the predictor effects to the rolling moment coefficient into following groups:

Large effect terms:	$\beta\alpha^3$	$\beta\alpha^2$	$\beta\alpha$		
	$\delta_{FA}\alpha^2$	$\delta_{FA}\alpha$	$\delta_{HTA}\alpha^2$	$\delta_{HTA}\alpha$	
	$\delta\alpha^2$	$p\alpha$	$p\alpha^2$	$r\alpha^2$	$r\alpha$
Small effect terms:	$\delta_{VC}\alpha^2$	$\delta_{VC}\alpha$			
	$\delta_{HTA}\delta_{FC}^2$	$\delta_{HTA}\delta_{FC}$	$(\delta_{FA}\delta_{FC}^2)$	$(\delta_{FA}\delta_{FC})$	
	$\beta\delta_{SP}$	$\beta\delta_{FC}$			
Insignificant terms:	$\delta r\delta_{FC}$	$\delta_{VC}\beta$	$\delta_{HTA}\delta_{FC}$		

$(\cdot)$ = not examined

Guidelines used to delineate the groups were based in part on the asymmetrical flap deflection. It was decided that a good threshold for determining a predictor's significance to the rolling moment would be the amount of rolling moment caused by one degree of asymmetical flap deflection (with α and β both at zero degrees). This level was -2.25 E-3; at the chosen design flight condition. Thus if any predictor, over the full range of the independent variable, did not display a difference in rolling moment of greater than | -2.25 E-3 |, then that predictor was deemed insignificant. Since differentiating between large and small only serves to set the order by which the predictor terms are tried in the regression analysis (in case the computer cannot handle all the predictors at once) and does not eliminate any predictor terms, the actual cutoff level chosen is not that important. An arbitrary level of 1.0 E-2 (approximately 5 times the one degree flap effectiveness) was set as the cutoff between large and small predictor terms.

In addition to these predictor terms, those terms from [8] that are consistent with the quasi-linear model were added, viz.

$$\beta^2, \beta^3, \beta^4, \beta^5, \beta^3\alpha^2, \beta^3\alpha \quad .$$

Because the analysis method depends on visual interpretation of the plots, limits to the number of cross variables with high orders that can be detected are inherent in the method. Also, in the case of single, high ordered variable predictors, plots similar to those made for two different variables were not possible (e.g., a sensitivity plot of the coefficient of rolling moment due to β as a function of β^2). However, it was possible to rule out the suggested predictors, β^4 and β^5 (because none of the C_l versus β plots indicated any discernible high ordered characteristics). After adding the seven lateral axis, linear predictors (i.e., first ordered, single, independent variables, ψ) from the linear model, thirty-one predictor terms were present to be tested in the regression analysis. These terms were:

β, p, r, δ_r, δ_{HTA}, δ_{FA}, δ_{VC}

$\beta\alpha^3$	$\beta\alpha^2$	$\beta\alpha$	$\beta\delta_{SP}$	$\beta\delta_{FC}$	$\delta_{HTA}\delta_{FC}^2$	$\delta_{HTA}\delta_{FC}$	$\delta_{FA}\delta_{FC}^2$	$\delta_{FA}\delta_{FC}$
$\delta_{HTA}\alpha^2$	$\delta_{HTA}\alpha$	$\delta_{FA}\alpha^2$	$\delta_{FA}\alpha$	$\delta_{VC}\alpha^2$	$\delta_{VC}\alpha$	$\delta_r\alpha$	$p\alpha^2$	$p\alpha$
$r\alpha^2$	$r\alpha$	$\beta^3\alpha^2$	$\beta^3\alpha$	β^3	β^2			

Step 4 - Perform backward elimination regression analysis

Before any regression analysis could be implemented, the dependent variables, the non-dimensional aerodynamic coefficient of rolling moment, had to be generated. To generate these non-dimensional coefficients, an AFTI/F-16 aerodynamic package supplied by NASA was used. The software package is based on look-up tables and is comprised of two parts. The first part is an initialization routine that reads in all the tables from a data file. The second part is a routine that reads in twenty input parameter values (these include independent variables, causal variables, and other constants nescessary to drive the program), computes the aircraft

non-dimensional coefficients with the help of look-up tables, and outputs eight coefficients. The twenty inputs to the latter part of the simulation, REFAERO, are:

DYNAMIC INPUTS

Angle of Attack, Arctan (W/U)	Rad
Sideslip Angle, Arcsin (V/VTOT)	Rad
Mach Number	N.D.
Total True Airspeed	Ft/Sec
Pressure Altitude	Ft
Height of aircraft C.G. above runway	Ft
Euler Pitch Angle	Rad
Rudder Deflection (+ T.E.L.)	Deg
Left Horizontal Tail (+ T.E.D.)	Deg
Right Horizontal Tail (+ T.E.D.)	Deg
Speed Brakes, (0., 60.), (+ T.E.D.)	Deg
Left Trailing Edge Flap (+ T.E.D.)	Deg
Right Trailing Edge Flap (+ T.E.D.)	Deg
Left Vertical Canard (+ T.E.L.)	Deg
Right Vertical Canard (+ T.E.R.)	Deg
Sym Leading Edge Flaps (+ L.E.D.)	Deg
Deflection About Hinge Line	
Gear Deflection, 0. = Full Up, 1. = Full Down	
X Comp of Rotat Vel	Rad/Sec
Y Comp of Rotat Vel	Rad/Sec
Z Comp of Rotat Vel	Rad/Sec

The standard six degree-of-freedom nondimensional coefficients [10] plus two additional coefficients to account for the effects of the angle-of-attack rate on longitudinal forces and moments comprise the output:

OUTPUTS - BODY FRAME

X Comp of Steady Flow Aero Force
Y Comp of Steady Flow Aero Force
Z Comp of Steady Flow Aero Force
X Comp of Steady Flow Aero Moment
Y Comp of Steady Flow Aero Moment
Z Comp of Steady Flow Aero Moment
D(C Lift)/D(CBar*Alphadot/2*Vtot)
D(C Pitch)/D(CBar*Alphadot/2*Vtot)

For this study, which develops the rolling moment only to show the feasibility of an expanded envelope residual generator, the requirements for the input and output were less numerous. As mentioned earlier in the development of the approach, the quasi-linear model (also referred to as the "nonlinear model") approach may eventually depend on using multiple models scheduled to the Mach number; therfore, each model must be based on a fixed Mach number. As a result, all data generated by the simulation for this modeling effort were based on one Mach number. In addition, other parameters that were deemed inconsequential to the study or outside the scope of the study were held fixed. In effect, the aircraft was simulated at one "flight condition" with no limit to its inertial rates or command deflections. Seven parameters were fixed at constant values:

FIXED VALUES

	Constant Value
Mach #	.6
V_T	660.
Altitude	15000.
Runway Altitude	1000.
Flight Path Angle	0.
δ_{SB}	0.
δ_{GEAR}	0.

The remaining thirteen parameters were driven by a random number generator resident on the VAX 11-750, varying within the physical limits of the aircraft (deflection limits) or within reasonable values encountered during evasive maneuvers (alpha, beta, angular rates). Some of the limits were later additionally confined by decisions made in selecting the potential terms (see subsection 4.1.2, step 3). The list below gives the original physical limits set on the aircraft parameters and their succeeding modifications.

SAMPLED VALUES

	min	max	
α	-.174533	.523599	radians
β	-.087267 -.043633	.087267 .04363	radians (original) radians (modified)
δr	-30. -20.	20. 20.	degrees (original) degrees (modified)
δ_{HTL}	-25.	25.	degrees
δ_{HTR}	-25.	25.	degrees
δ_{FL}	-21.5	21.5	degrees
δ_{FR}	-21.5	21.5	degrees
δ_{VCL}	-27. -15.	27. 15.	degrees (original) degrees (modified)
δ_{VCR}	-27. -15.	27. 15.	degrees (original) degrees (modified)
δ_{LEF}	-2.43	29.58	degrees
p	-3.49	3.49	radians/sec.
q	-.175	.175	radians/sec.
r	-.436	.436	radians/sec.

where

V_T	Total Air Speed
δ_{SB}	Speed Brake
δ_{GEAR}	Landing Gear
δ_r	Rudder
δ_{HTL}	L. Horizontal Tail
δ_{HTR}	R. Horizontal Tail
δ_{FL}	L. Flap
δ_{FR}	R. Flap
δ_{VCL}	L. Canard
δ_{VCR}	R. Canard
δ_{LEF}	Leading Edge Flap

In all, 1000 samples of these thirteen parameters were generated to represent the sample space of all possible combinations. More details on the sampling issue will be discussed in subsection 4.1.4.

After the dependent variables had been generated, a regression analysis was used to choose the quasi-linear predictor terms of the polynomial. The regression process was a backward elimination regression [5] with the following criteria for removing terms from the polynomial:

1. A significance threshold was computed to represent the minimum level of contribution to the non-dimensional rolling moment coefficient that a predictor term should have. In general, the greatest control surface influence to the rolling moment is the effects of the aileron, or in the case of the AFTI F-16, the flaperons. Thus, for this case, the significance threshold was set equal to one degree of asymmetrical flaperon deflection. Therefore, if a "typically large" value of a predictor (could be multiple variables, higher order variables, or both) multiplied by its coefficient contributes less to the non-dimensional rolling moment coefficient than 1 degree of asymmetrical flap deflection, then that predictor term was deemed insignificant and dropped from the polynomial. The "typically large" values chosen to represent the variables were:

α	0.52	radians
β	0.044	radians
p	3.50	radians/sec
r	0.44	radians/sec
δr	20.0	degrees
δ_{HTL} or δ_{HTR}	25.0	degrees
δ_{FL} or δ_{FR}	21.5	degrees
δ_{VCL} or δ_{VCR}	15.0	degrees

The threshold level for significance, that is, the non-dimensional rolling moment coefficient for one degree of asymmetrical flap (as determined from the first regression run) was $C_l = -1.785$ E-3.

2. It was decided that the error standard deviation (variance)for the original, nonlinear set of predictors (31 terms) should not deteriorate by more than 10% (21%). Computation of the sample variance of the predicted error in the residual is given by (see Section 2)

$$FOM^2 = \frac{1}{n-1}\left[y^T y + a_s^T\left(X_s^T X_s\right)a_s - 2a_s^T\left(X_s^T y\right) + \sigma_y^2 + a_s^T \Sigma_s a_s\right] \qquad (4\text{-}7)$$

where a_s and X_s are scaled versions of the vector a and the matrix X, as described in Eq. 2-13 (scaling is discussed in subsection 4.1.4.

The above two criteria were applied until either all remaining predictor terms complied with the first critierion or until the FOM (the prediction-error variance) of the latest regression run had exceeded the ten percent limit.

Linear Model

The linear case was developed to provide a standard for comparison to the nonlinear cases. The sample-variance of the model prediction-error for the linear case was 4.53495 E-5 (standard deviation of about 6.7342 E-3).

The resulting linear model was

$$\begin{aligned} C_l &= C_{l_\beta}\cdot\beta + \frac{b}{2V_T}C_{l_p}\cdot p + \frac{b}{2V_T}C_{l_r}\cdot r \\ &+ C_{l_{\delta_r}}\cdot\delta_r + C_{l_{\delta_{HTA}}}\cdot\delta_{HTA} + C_{l_{\delta_{FA}}}\cdot\delta_{FA} + C_{l_{\delta_{VC}}}\cdot\delta_{VC} \\ &= (\text{-}1.03\text{E-}1)\,\beta + (\text{-}7.36\text{E-}3)\,p + (9.08\text{E-}4)\,r \\ &+ (2.02\text{E-}4)\,\delta_r + (\text{-}1.41\text{E-}3)\,\delta_{HTA} + (\text{-}1.44\text{E-}3)\,\delta_{FA} + (3.77\text{E-}5)\,\delta_{VC} \qquad (4\text{-}8) \end{aligned}$$

Nonlinear Model

The nonlinear regression required many iterations of the backward elimination procedure until one of the criteria was violated. The final form of the nonlinear equation contains 22 terms, six of which are linear terms. Table 4-2 shows the evolution of the regression analysis. As each term was removed from the polynomial, the loss of accuracy of the FOM was small.

TABLE 4.2

Trial Number	Number of Terms	FOM^2	Step Taken
1	31	5.5482 E-6	remove β^2
2	30	5.5489 E-6	remove β^3
3	29	5.5507 E-6	remove $\beta\ \delta_{FC}$
4	28	5.5578 E-6	remove $\beta^3\ \alpha^2$
5	27	5.5577 E-6	remove $\beta^3\ \alpha$
6	26	5.5593 E-6	remove $\beta\ \delta_{SP}$
7	25	5.5737 E-6	remove r
8	24	5.7051 E-6	remove $\delta_{HTA}\ \delta_{FC}^2$
9	23	5.7052 E-6	remove δ_{VC}
10	22	5.8646 E-6	remove $\delta_{FA}\ \delta_{FC}^2$
11	21	5.8646 E-6	add δ_{VC}
12	22	5.7059 E-6	keep model

The removal of δ_{VC} did produce a larger relative increase of the FOM than any of the other terms, including the last one. Thus δ_{VC} was retained even though its maximum effect was below the one degree of flap threshold. This choice returned favorable results because the FOM with δ_{VC} was actually lower than the FOM without from the previous iteration.

The full 31-term model is:

$$
\begin{aligned}
C_l = {} & \text{-9.59E-02}\,\beta + \text{-8.15E-03}\,p + \text{-2.02E-03}\,r + \text{5.03E-04}\,\delta_r \\
& + \text{-1.58E-03}\,\delta_{HTA} + \text{-1.77E-03}\,\delta_{FA} + \text{8.84E-05}\,\delta_{VC} + \text{-1.004}\,\beta\alpha^3 \\
& + \text{0.775}\,\beta\alpha^2 + \text{-0.216}\,\beta\alpha + \text{7.78E-04}\,\beta\delta_{SP} + \text{-3.67E-04}\,\beta\delta_{FC} \\
& + \text{6.46E-03}\,\delta_{FA}\alpha^2 + \text{-5.59E-04}\,\delta_{FA}\alpha + \text{7.46E-08}\,\delta_{FA}\delta_{FC}^2 + \text{2.67E-05}\,\delta_{FA}\delta_{FC} \\
& + \text{6.15E-03}\,\delta_{HTA}\alpha^2 + \text{-1.43E-03}\,\delta_{HTA}\alpha + \text{-1.23E-08}\,\delta_{HTA}\delta_{FC}^2 + \text{2.51E-06}\,\delta_{HTA}\delta_{FC} \\
& + \text{-1.68E-03}\,\delta_r\alpha + \text{-6.61E-03}\,p\alpha^2 + \text{6.66E-03}\,p\alpha + \text{1.37E-03}\,\delta_{VC}\alpha^2 \\
& + \text{-9.06E-04}\,\delta_{VC}\alpha + \text{-1.94E-02}\,r\alpha^2 + \text{2.32E-02}\,r\alpha + \text{-26.43}\,\beta^3\alpha^2 \\
& + \text{8.678}\,\beta^3\alpha + \text{4.28}\,\beta^3 + \text{1.86E-02}\,\beta^2 \qquad (4\text{-}9)
\end{aligned}
$$

The final 22-term polynomial equation for the nonlinear model is:

$$
\begin{aligned}
C_l = {} & (-8.97E\text{-}2)\,\beta + (-8.17E\text{-}3)\,p + (5.05E\text{-}4)\,\delta_r + (-1.58E\text{-}3)\,\delta_{HTA} \\
& + (-1.77E\text{-}3)\,\delta_{FA} + (9.03E\text{-}5)\,\delta_{VC} + (-9.35E\text{-}1)\,\beta\alpha^3 + (7.05E\text{-}1)\,\beta\alpha^2 \\
& + (-2.03E\text{-}1)\,\beta\alpha + (6.45E\text{-}3)\,\delta_{FA}\alpha^2 + (-5.54E\text{-}4)\,\delta_{FA}\alpha + (2.67E\text{-}5)\,\delta_{FA}\delta_{FC} \\
& + (6.11E\text{-}3)\,\delta_{HTA}\alpha^2 + (-1.42E\text{-}3)\,\delta_{HTA}\alpha + (2.45E\text{-}6)\,\delta_{HTA}\delta_{FC} + (-1.68E\text{-}3)\,\delta_r\alpha \\
& + (-6.51E\text{-}3)\,p\alpha^2 + (6.64E\text{-}3)\,p\alpha + (1.45E\text{-}3)\,\delta_{VC}\alpha^2 + (-9.39E\text{-}4)\,\delta_{VC}\alpha \\
& + (-2.42E\text{-}2)\,r\alpha^2 + (1.98E\text{-}3)\,r\alpha \qquad (4\text{-}10)
\end{aligned}
$$

The final FOM for the 22-term nonlinear model was 2.39 E-3, which is a 64 percent reduction in the standard deviation of the residual model error as compared to the linear model FOM of 6.73 E-3. This model produces a significant inprovement in the predicted error of the residual over the linear model. This model also reflects a relatively small loss in accuracy compared to the full 31-term case, which had a FOM of 2.35 E-3. Recall that the FOM is a measure of model error, and the goal is to minimize the FOM.

The 22-term model's standard deviation of 2.39 E-3 is roughly one and one-third times the one degree of differential flap level of -1.78 E-3 (based on the final model), a good improvement over the factor of four from the linear models' corresponding ratio of standard deviation to significance threshold.

4.1.3 Incorporating Sensor Noise In The Rolling Moment Model

As detailed in subsection 2.2.3, the quasi-linear regression incorporates the impact of sensor noises. The original intent in the development of the sensor noise-incorporated rolling moment model was to reduce the regression analysis to one step, that is, given the original set of 31 predictors, the optimal solution can be readily determined from the regression coefficients output from the 31 predictor run. Unfortunately, the implementation for the generation of Σ (in Eq. 2-12) is not a trivial one. Due to time constraints and computational requirements, the computation of Σ was not used to finalize the models (that is, the Σ matrix was set to zero). Its impact is now discussed. The Σ matrix is defined as:

$$\Sigma_{ij} = E(W_i W_j) \tag{4-11}$$

where

$$W_i = X_i^m - X_i$$

For each individual component of Σ, the expanded term will be a polynomial. This polynomial consists of terms, all of which have at least one variable as part of the term with the exception of the noise only term. If we assume that all variables have zero mean, then when the expected value is taken, all individual terms of each polynomial will have at least one variable to reduce that term to zero, with the exception of the one term with all noise variables. Thus, the sigma array would consist of components that contain one term each. These terms are in the form of

$$\eta_a^i \, \eta_b^j.$$

Many of these terms are actually a combination of two or more measurements and thus also, two or more noise values, e.g.,

$$\delta_{FC} + \eta_{FC} = 1/2 * (\delta_{FL} + \eta_{FL} + \delta_{FR} + \eta_{FR}) \tag{4–12}$$

where,

FC = collective flaperon

FL = left flaperon

FR = right flaperon

For these terms, which can all be written in the form $(a+b)^k$, the expansion of the polynomial will result in no terms that are all even-ordered if k is odd. (For this specific set of terms, all cross terms will result in n being an odd number.) Since all odd moments of a Gaussian distribution have zero mean, those terms that are not all even-ordered can be ignored [7], viz., given that a variable X has a normal probability density,

$$E\left[(x-m)^k\right] = \begin{cases} 1 \times 3 \times 5 \ldots (k-1)\,\sigma^k & \text{for k even} \\ 0 & \text{for k odd} \end{cases} \tag{4-13}$$

where

$$m = \text{mean} = E[X]$$

$$\sigma^2 = \text{var}[X]$$

Therefore, although there are combination terms like the deflections, they can be treated as any other measured variables. As an example of the Σ derivation, let

$$X_1 = (\alpha\beta)$$

$$X_1^m = \alpha\beta + \underbrace{\eta_\alpha\beta + \alpha\eta_\beta + \eta_\alpha\eta_\beta}_{\eta_1}$$

$$X_2 = \beta$$

$$X_2^m = \beta + \underbrace{\eta_\beta}_{\eta_2} \qquad (4\text{-}14)$$

$$S_{12} = E(\eta_1\eta_2) = E\left[\eta_\alpha\eta_\beta \cdot \beta + \alpha\eta_\beta^2 + \eta_\alpha\eta_\beta^2\right]$$

In addition to the assumptions made above for sigma, simplifications had to be made to the cross terms of the Σ matrix. These simplifications were made because of the complexity of implementing symbolic manipulation, which was required to solve the polyomials of the cross terms. Instead, it was decided to just model the cross term effects as insignificant compared to the diagonal terms. The resulting Σ matrix will have the form:

$$\Sigma = \begin{bmatrix} E(\eta_1\eta_1) & & 0 \\ & E(\eta_2\eta_2) & \\ & & \ddots \\ 0 & & E(\eta_n\eta_n) \end{bmatrix} \qquad (4\text{-}15)$$

The diagonal terms of the Σ matix are given in Table 4-3.

TABLE 4-3. DIAGONAL TERMS OF THE Σ MATRIX

	TERM	(ASSUMES ALL MEANS OF VARIABLES = 0)	$E(\eta^2)$
1	β	η_β	σ^2_β
2	p	η_{pb}	σ^2_{pb}
3	r	η_{rb}	σ^2_{rb}
4	δ_r	η_r	σ^2_r
5	δ_{HTA}	$\frac{1}{2}(\eta_{TR}-\eta_{TL})$	$\frac{1}{4}(\sigma^2_{TR}+\sigma^2_{TL})$
6	δ_{FA}	$\frac{1}{2}(\eta_{FR}-\eta_{FL})$	$\frac{1}{4}(\sigma^2_{FR}+\sigma^2_{FL})$
7	δ_{CA}	$\frac{1}{2}(\eta_{CL}-\eta_{CR})$	$\frac{1}{4}(\sigma^2_{CL}+\sigma^2_{CR})$
8	$\beta\alpha^3$	$\eta_\beta\eta_\alpha{}^3$	$15\,\sigma^2_\beta\sigma^6_\alpha$
9	$\beta\alpha^2$	$\eta_\beta\eta_\alpha{}^2$	$3\,\sigma^2_\beta\sigma^4_\alpha$
10	$\beta\alpha$	$\eta_\beta\eta_\alpha$	$\sigma^2_\beta\sigma^2_\alpha$
11	$\beta\delta_{CC}$	$\eta_\beta\frac{1}{2}(\eta_{CL}+\eta_{CR})$	$\frac{1}{4}\sigma^2_\beta(\sigma^2_{CR}+\sigma^2_{CL})$
12	$\beta\delta_{FC}$	$\eta_\beta\frac{1}{2}(\eta_{FR}+\eta_{FL})$	$\frac{1}{4}\sigma^2_\beta(\sigma^2_{FR}+\sigma^2_{FL})$
13	$\delta_{FA}\alpha^2$	$\frac{1}{2}(\eta_{FR}-\eta_{FL})\eta^2_\alpha$	$\frac{3}{4}(\sigma^2_{FR}+\sigma^2_{FL})\,\sigma^4_\alpha$
14	$\delta_{FA}\alpha$	$\frac{1}{2}(\eta_{FR}-\eta_{FL})\eta_\alpha$	$\frac{1}{4}(\sigma^2_{FR}+\sigma^2_{FL})\,\sigma^2_\alpha$
15	$\delta_{FA}\delta^2_{FC}$	$\frac{1}{8}(\eta_{FR}-\eta_{FL})\,(\eta_{FR}+\eta_{FL})^2$	$\frac{1}{64}(15\sigma^6_{FR}-3\sigma^4_{FR}\sigma^2_{FL}-3\sigma^2_{FR}\sigma^4_{FL}+15\sigma^6_{FL})$
16	$\delta_{FA}\delta_{FC}$	$\frac{1}{4}(\eta_{FR}-\eta_{FL})\,(\eta_{FR}+\eta_{FL})$	$\frac{1}{16}(3\sigma^4_{FR}-2\sigma^2_{FR}\sigma^2_{FL}+3\sigma^4_{FR})$
17	$\delta_{HTA}\alpha^2$	$\frac{1}{2}(\eta_{TR}-\eta_{TL})\,\eta^2_\alpha$	$\frac{3}{4}(\sigma^2_{TR}+\sigma^2_{TL})\,\sigma^4_\alpha$
18	$\delta_{HTA}\alpha$	$\frac{1}{2}(\eta_{TR}-\eta_{TL})\,\eta_\alpha$	$\frac{1}{4}(\sigma^2_{TR}+\sigma^2_{TL})\,\sigma^2_\alpha$
19	$\delta_{HTA}\delta^2_{FC}$	$\frac{1}{8}(\eta_{TR}-\eta_{TL})\,(\eta_{FR}+\eta_{FL})^2$	$\frac{1}{16}(\sigma^2_{TR}+\sigma^2_{TL})\,(3\sigma^4_{FR}+3\eta^2_{FR}\eta^2_{FL}+3\eta^4_{FL})$
20	$\delta_{HTA}\delta_{FC}$	$\frac{1}{4}(\eta_{TR}-\eta_{TL})\,(\eta_{FR}+\eta_{FL})^2$	$\frac{1}{4}(\sigma^2_{TR}+\sigma^2_{TL})\,(\sigma^2_{FR}+\sigma^2_{FL})$
21	$\delta_r\alpha$	$\eta_r\eta_\alpha$	$\sigma^2_r\sigma^2_\alpha$
22	$p\alpha^2$	$\eta_{pb}\eta^2_\alpha$	$3\sigma^2_{pb}\sigma^4_\alpha$
23	$p\alpha$	$\eta_{pb}\eta_\alpha$	$\sigma^2_{pb}\sigma^2_\alpha$
24	$\delta_{CA}\alpha^2$	$(\eta_{CL}-\eta_{CR})\,\eta^2_\alpha$	$3(\sigma^2_{CR}+\sigma^2_{CL})\,\sigma^4_\alpha$
25	$\delta_{CA}\alpha$	$(\eta_{CL}-\eta_{CR})\,\eta_\alpha$	$(\sigma^2_{CR}+\sigma^2_{CL})\,\sigma^2_\alpha$
26	$r\alpha^2$	$\eta_{rb}\eta^2_\alpha$	$3\sigma^2_{rb}\sigma^4_\alpha$
27	$r\alpha$	$\eta_{rb}\eta_\alpha$	$\sigma^2_{rb}\sigma^2_\alpha$
28	$\beta^3\alpha^2$	$\eta^3_\beta\eta^2_\alpha$	$15\sigma^6_\beta\sigma^4_\alpha$
29	$\beta^3\alpha$	$\eta^3_\beta\eta_\alpha$	$15\sigma^6_\beta\sigma^2$
30	β^3	η^3_β	$15\sigma^6_\beta$
31	β^2	η^2_β	$3\sigma^4_\beta$

R-6568

The sensor values that were used for this study were sensor values from an old Boeing 737 model. These are listed below:

α:	0.007	radians
β:	0.007	radians
p:	0.00035	radians
r:	0.00035	radians
δ_{FL}:	0.1	degrees
δ_{FR}:	0.1	degrees
δ_{HTL}:	0.1	degrees
δ_{HTR}:	0.1	degrees
δ_{VCL}:	0.1	degrees
δ_{VCR}:	0.1	degrees
δr:	0.1	degrees

Linear and nonlinear models were also generated with the sensor noises incorporated into the computations. The linear model with sensor noises incorporated resulted in an FOM of 6.7 E-3. The equation for this model is:

$$\begin{aligned} CLB = {} & (-1.03153E\text{-}1)\,\beta + (-7.37007E\text{-}3)\,p + (9.09075E\text{-}4)\,r + (2.02038E\text{-}4)\,\delta_r \\ & + (-1.41048E\text{-}3)\,\delta_{HTA} + (-1.44512E\text{-}3)\,\delta_{FA} + (3.76989E\text{-}5)\,\delta_{VC} \end{aligned} \quad (4\text{-}16)$$

The nonlinear model (22 predictor terms) with the addition of sensor noises showed comparable relative changes to those of the linear model. The FOM was 2.39 E -3 and the polynomial equation for C_l was:

$$\begin{aligned} CLB = {} & -8.97E\text{-}02\,\beta + -8.17E\text{-}03\,p + 5.05E\text{-}04\,\delta r + -1.58E\text{-}03\,\delta_{HTA} \\ & + -1.77E\text{-}03\,\delta_{FA} + 9.03E\text{-}05\,\delta_{VC} + 0.934\,\beta\alpha^3 + 0.704\,\beta\alpha^2 \\ & + -0.203\,\beta\alpha + 6.45E\text{-}03\,\delta_{FA}\alpha^2 + -5.54E\text{-}04\,\delta_{FA}\alpha + 2.67E\text{-}05\,\delta_{FA}\delta_{FC} \\ & + 6.11E\text{-}03\,\delta_{HTA}\alpha^2 + -1.42E\text{-}03\,\delta_{HTA}\alpha + 2.45E\text{-}06\,\delta_{HTA}\delta_{FC} + 1.68E\text{-}03\,\delta_r\alpha \\ & + -6.51E\text{-}03\,p\alpha^2 + 6.64E\text{-}03\,p\alpha + 1.45E\text{-}03\,\delta_{VC}\alpha^2 + -9.39E\text{-}04\,\delta_{VC}\alpha \\ & + 2.42E\text{-}02\,r\alpha^2 + 1.92E\text{-}02\,r\alpha \end{aligned} \quad (4\text{-}17)$$

The full nonlinear model with 31-terms and sensor noise calculations is

$$
\begin{aligned}
CLB = {} & -9.58E\text{-}02\,\beta + -8.15E\text{-}03\,p + -2.02E\text{-}03\,r + 5.03E\text{-}04\,\delta_r \\
& + -1.58E\text{-}03\,\delta_{HTA} + -1.77E\text{-}03\,\delta_{FA} + 8.84E\text{-}05\,\delta_{VC} + -1.003\,\beta\alpha^3 \\
& + 0.774\,\beta\alpha^2 + -0.216\,\beta\alpha + 7.78E\text{-}04\,\beta\delta_{SP} + -3.67E\text{-}04\,\beta\delta_{FC} \\
& + 6.46E\text{-}03\,\delta_{FA}\alpha^2 + -5.59E\text{-}04\,\delta_{FA}\alpha + 7.46E\text{-}08\,\delta_{FA}\delta_{TC}^2 + 2.67E\text{-}05\,\delta_{FA}\delta_{TC} \\
& + 6.15E\text{-}03\,\delta_{HTA}\alpha^2 + -1.43E\text{-}03\,\delta_{HTA}\alpha + -1.22E\text{-}08\,\delta_{HTA}\delta_{FC}^2 + 2.51E\text{-}06\,\delta_{HTA}\delta_{FC} \\
& + -1.68E\text{-}03\,\delta_r\alpha + -6.61E\text{-}03\,p\alpha^2 + 6.66E\text{-}03\,p\alpha + 1.37E\text{-}03\,\delta_{VC}\alpha^2 \\
& + -9.06E\text{-}04\,\delta_{VC}\alpha + -1.94E\text{-}02\,r\alpha^2 + 2.32E\text{-}02\,r\alpha + -26.26\,\beta^3\alpha^2 \\
& + 8.771\,\beta^3\alpha + 4.21\,\beta^3 + 1.86E\text{-}02\,\beta^2 \qquad (4\text{-}18)
\end{aligned}
$$

4.1.4 Computational Issues

To run the regression analysis on the suspected terms, non-dimensional, aerodynamic coefficients first must be generated. This output should be representative of the full range of the aircraft control inputs and inertial outputs throughout the flight envelope. With thirteen input parameters that are varied, a factorial design (all combinations of all levels of each parameter) is not feasible. Therefore, the sample inputs that are generated must be well distributed over the sample space. This section addresses the issue of generating truly random samples for the aerodynamic package and the associated problems of producing well conditioned random arrays.

For each run of the regression analysis, one thousand samples or sets of input were generated by an accompanying program to the aerodynamic program. The number of samples chosen per run was originally limited to 10,000 samples by the hardware limitations of the VAX internal storage size. Ideally, a minimum of a factorial sample is desired, that is, a sample large enough to cover every possible combination of variables, given a predetermined, discrete interval for each variable. However, this was not possible and later, due to run-time constraints, the number of samples was reduced to 1000 (which produced very good response time). To insure that the sample space over the thirteen variables was representative,

uniformity checks were made for both the random number seed and for the actual samples that were generated.

The impetus for testing the random number seed and the random number generator on the VAX 11-750 was based on suspicions that although each parameter could show uniformity along its range, that it was still possible that correlation could still exist between the parameters or channels. For example, though random numbers for alpha and beta could be evenly distributed individually along their full range, nothing precluded all low values of alpha being generated when all low values of beta were being generated, and vice versa for the high values. Thus, uniformity along n-factorial space was also desired. One method for checking non-correlation of values is detailed in [11]. This method uses counters for each "factorial space" and computes a chi-square value:

Let U_i's be random values [0,1]

Let $U_1 = (U_1, U_2, ..., U_d)$

$U_2 = (U_{d+1}, U_{d+2}, ..., U_{2d})$

$$K^2(d) = \frac{K^d}{n} \sum_{j_1=1}^{K} \sum_{j_2=1}^{K} \cdots \sum_{j_d=1}^{K} \left(f_{j_1 j_2 \cdots j_d} - \frac{n}{K^d} \right)^2 \qquad (4\text{-}19)$$

where

K = # of subintervals in [0,1]

d = # of dimensions (variables)

n = # of samples

$f_{j1j2...jd}$ = Ui's having first component in subinterval j1 and second component in subinterval j2, etc.

Using the above test for n=3 channels, various random number seeds (some were ones suggested by [11], others were arbitrarily picked) were evaluated. The random number seed that gave the most favorable result was 8374997 which had chi-square = 4021, where 4095 was the upper limit for a well-behaved random number generator seed. In general, the smaller chi-square is, the better the seed value is. The test was repeated for the same seed at n=5

channels and only 10 gradations per channel as opposed to 16 gradations for the previous test. The resulting chi-square value, 100,234 , was slightly higher than the suggested upper limit, 99,999. One explanation for the higher values could be the reduction in the fineness of the gradations.

One interesting note discovered during the random number seed tests was that the random numbers are highly correlated if used sequentially along a variable. That is, if the sequentially generated numbers are distributed down the first variable before being distributed down the second variable, etc., as opposed to distributing the numbers across all variables, one number per variable. For the case where the numbers are all generated down one variable before another, the chi-square value for a three variable case was 330,722.5, where 4095 was the acceptable upper limit. In addition to testing the random number generator resident on the VAX, a Tausworthe generator was implemented as an alternative (see [11]). Although it showed promise with respect to lack of correlation, the speed of the generator (more than five times slower) made it prohibitively impractical to use or even evaluate extensively.

After the random number seed was selected, a second test for uniformity was done on the actual input array of random numbers generated. (Due to the hardware constraints of the VAX, the chi-square test could not test the chosen seed for the thirteen variable case.) The input array was a 1000 x 13 array of random numbers between 0.0 and 1.0 called X_{seed}. The pseudo-inverse of X_{seed} was taken (more specifically, $X_{seed}{}^{t}X_{seed}$ was checked for singularity) to see if it was well conditioned. To determine whether the array was well-conditioned, singular value decomposition was utilized to examine the condition number. This number is a ratio of the largest value to the smallest singular value. The resulting condition number from this verification was 42.66, well within working precision limits.

Although the sampled array (13 input variables with values [0,1] X 1000 points) generated by the random number generator was well conditioned, the resulting scaled $X^{t}X$ array was not. The scaled $X^{t}X$ array contains the random values adjusted to the minimum and maximum ranges of each individual variable. Due to the large storage demands of processing

such large arrays, the code had to be implemented in single precision. This limited working precision caused the X^tX to appear singular during the inversion process. Using X^tX in the solution method when the array is singular further compunds the problem of an ill-scaled X array. While methods do exist for avoiding the pseudo-inverse (such as the LDU method, QR method, [12]), it was still preferable to use X^tX, if possible, because of the heavy memory requirements associated with storing X (X need not be stored to compute X^tX). In addition, the form X^tX is required in the sensor computations described above (see subsection 4.1.3). Therefore, the goal was to get X as well conditioned as possible through scaling of the columns. This was achieved through the following procedure.

Let x = [mxn] array , a = coefficient vector [nx1]. Instead of X, use $X_S = Xd$ and $a_S = d^{-1}a$ where d = diagonal scaling matrix. Then

$$\begin{aligned} y = Xa = (Xd)\,(d^{-1}a) &= X_S a_S \\ (X_S^T X_S)\, a_S &= X_S^T y \\ a_S &= [X_S^T X_S]^{-1} X_S^T y \\ a &= d[X_S^T X_S]^{-1} X_S^T y \end{aligned} \qquad (4\text{-}20)$$

For the case using Σ,

$$a = d(X_S^T X_S + \Sigma_S)^{-1} X_S^T y \qquad (4\text{-}21)$$

where

$$\Sigma_S = d^T \Sigma d \ .$$

For determining which variables to scale and by how much, the heuristic used was to scale by factors of ten so that all the X^tX diagonal elements were within an order of magnitude from each other. The scaling factors that were chosen are given below:

1	β	.1	8	$\beta\alpha^3$	100
2	p	.1	9	$\beta\alpha^2$	100
3	r	.1	10	$\beta\alpha$	100
4	δ_r	.01	11	$\beta\delta_{SP}$	1
5	δ_{HTA}	.01	12	$\beta\delta_{FC}$	1
6	δ_{FA}	.1	13	$\delta_{FA}\alpha^2$	1
7	δ_{VC}	.1	14	$\delta_{FA}\alpha$	0.1

15	$\delta_{FA}\delta_{FC}^2$	0.001	24	$\delta_{VC}\alpha^2$	1
16	$\delta_{FA}\delta_{FC}$	0.01	25	$\delta_{VC}\alpha$	0.1
17	$\delta_{HTA}\alpha^2$	0.1	26	$r\alpha^2$	10
18	$\delta_{HTA}\alpha$	0.1	27	$r\alpha$	10
19	$\delta_{HTA}\delta_{FC}^2$	0.0001	28	$\beta^3\alpha^2$	10^5
20	$\delta_{HTA}\delta_{FC}$	0.01	29	$\beta^3\alpha$	10^5
21	$\delta_r\alpha$	0.1	30	β^3	10^4
22	$p\alpha^2$	1	31	β^2	10^3
23	$p\alpha$	1			

4.2 RESIDUAL GENERATION -- IMPLEMENTATION

After the coefficients for the quasi-linear models have been produced, the process of generating the residuals can be completed. The purpose of this section is to describe the implementation of the residual generator. A residual generation program was implemented on the VAX 11-750 similar to the program that was created for the single flight condition residual generation from an earlier task [2]. The model for the aircaraft dynamics and kinematics used to create the residuals plus some preliminary calculations incorporated to prepare the flight data are given in subsection 4.2.1. The test plan for the simulations is outlined in subsection 4.2.2, and the test results and conclusions are presented in subsections 4.2.3 and subsections 4.2.4, respectively.

4.2.1 Residual Generation Equations

The general force and moment balance equations are given by

$$X = \bar{Q}S\,(CXB)$$
$$Y = \bar{Q}S\,(CYB)$$
$$Z = \bar{Q}S\,(CZB)$$
$$L = \bar{Q}Sb\,(CLB)$$
$$M = \bar{Q}S\bar{c}\,(CMB)$$
$$N = \bar{Q}Sb\,(CNB)$$

From the rolling moment, the CLB is obtained from one of the C_l models in subsection 4.1. The predicted angular acceleration along the X-axis can be computed as:

$$\hat{\dot{p}} = \left[\left(I_{yy} - I_{zz} \right) / I_{xx} \right] * r * q + L / I_{xx} \qquad (4\text{-}22)$$

Using the tapezoidal rule, with $\dot{p}$ computed from the present and previous roll rates, the residual is derived as:

$$\nu_p(k+1) = \dot{p}(k+1) - \frac{\hat{p}(k+1) + \hat{p}(k)}{2} \qquad (4\text{-}23)$$

The flight data that provides the measured deflections and also the aerodynamic values such as α, β, p, q, r, etc. are retrieved from sequential data generated from a simulation package that used REFAERO as the aerodynamic model. These simulation runs were generated by NASA based on the maneuvers listed in the test plan (subsection 4.2.2). To insure that the data had the proper units and format, the data was configured from its original form (binary, 97 channels) to a temporary form more readily accessible to the residual generator (ascii, 18 channels). Since the flight data was generated from the NASA simulation package, it represented the true aircraft states. To simulate the errors inherent in measurement, noise was added to the true data before it was passed to the residual generator.

4.2.2 Test Plan

The test plan calls for simulation runs using three different aircraft maneuvers. These three maneuvers were selected from typical maneuvers encountered during normal flight. It is expected that the three maneuvers will task the range of aircraft motions and required controls. The three maneuvers are shown in Table 4-4. These three maneuvers were tested over several flight conditions. These flight conditions were chosen by NASA as a representative range of conditions, with the intention of displaying the deficiencies of the linear model and the robustness of the nonlinear model. The flight conditions are:

Trim Condition	Altitude (feet)	Speed	Angle of Attack
F1	10,000	600 ft/sec	2.84
F2	2,500	Mach .2	18.82
F3	30,00	Mach 1.4	2.12

TABLE 4-4. TEST PLAN

Plane initially should be straight and level, p, q, r=0, constant velocity

		Time (secs)	Ramp Value (degrees/sec)	
M1 -	**Heading Change**			
	Navigational Maneuver	1.0	p = 180	q = 0
		1.5	p = 0	q = 10
		6.0	p = -180	q = 0
		6.5	p = 0	q = 0
		8.0	stop	
M2 -	**Peek and Dive**			
	Evasive Maneuver	1.0	p = 0	q = 20
		3.0	p = 0	q = 0
		6.0	p = 0	q = 20
		8.0	p = 360	q = 0
		8.5	p = 0	q = 20
		10.0	p = 180	q = 0
		11.0	p = 0	1 = 20
		12.5	p = 0	q = 0
		14.0	stop	
M3 -	**Climbing Turn**			
	Navigational Maneuver	1.0	p = 90	q = 10
		1.25	p = 0	q = 0
		6.25	p = -90	q = -10
		6.50	p = 0	q = 0
		8.0	stop	

In addition to making comparisons between the linear and nonlinear cases of the model with sensor noises included, runs will be made with the nonlinear model that doesn't incorporate predicted sensor noises to show the improvements when sensor noises are modeled. Table 4-5 summarizes the simulation runs that are planned.

TABLE 4-5. PLANNED SIMULATION RUNS

Trim Condition	Maneuver M1	Maneuver M2	Maneuver M3
F1	With Noise Without Noise	With Noise Without Noise	With Noise Without Noise
F2			With Noise Without Noise
F3	With Noise Without Noise	With Noise Without Noise	With Noise Without Noise

4.2.3 Results

As mentioned above, test runs were made using simulated flight data provided by NASA based on a full six degree-of-freedom nonlinear aerodynamic software package of the AFTI/F-16. This data was a best attempt at the prescribed maneuvers listed in the test plan, since no flight control system was available to implement exactly the desired aircraft maneuvers. For many of the following test comparisons, noise was added to the simulated flight data.

The results of the residual generation tests can be categorized into several areas and they will be examined in the following order: first, the benefits of the nonlinear model over a linear model are analyzed; then tradeoffs due to the reduction of terms will be discussed; next, comparisons of the effects of sensor noise modeling are made; and finally, performance of the models over several flight conditions are examined.

In general, it can be gathered that the reduced nonlinear model offers improved accuracy over the standard linear model and that the nonlinear model may use a reduced set of terms with no significant loss in accuracy. The incorporation of sensor noise computation produces

no discernible improvement in performance as long as the sensor noises are relatively small. And the nonlinear model performs well as long as operating conditions were fairly close to the modeled conditions.

Linear vs. Nonlinear models

To examine the benefits of using a nonlinear model as opposed to using a linear model, test runs were made with the linear model without sensor noise computations and the 22-term nonlinear model without sensor noise computations. Because the purpose of these comparisons were to look at the effects of using nonlinear predictor terms the two sets of runs were made without injecting Gaussian noise into the simulated flight data. The linear model and nonlinear models are the ones described in subsection 4.1.2 and are also labeled as Eqs. 4-8 and 4-10, respectively.

The flight condition selected for these runs, labeled as F1 from the previous section, most closely resembled the flight condition used to design the models. Although they are not identical (airspeed = 600 ft/sec., altitude = 10,000 ft vs. airspeed = 660 ft/sec., altitude = 15,000 ft) the flight conditions are similar enough to produce representative residuals. Figure 4-1 shows plots of the linear model residual versus the nonlinear model residual at flight condition F1 for each of the three maneuvers, M1, M2, and M3.

Recall that the FOM of the linear model was 6.73 E-3 and the FOM of the nonlinear model 2.39 E-3. From these values, dimensionalized FOMs for these two models can be computed. The expected standard deviation in the residual can be roughly approximated as

$$\bar{q}\ S\ b\ (FOM) / I_{XX} = \text{expected standard deviation of the residual, pdot} \qquad (4\text{-}24)$$

where,

$\bar{q}$ = dynamic pressure (lbs/ft^2)
S = surface area of wing (ft^2)
b = wingspan (ft)
I_{XX} = moment of inertia of the x axis (slugs-ft^2)

Thus, for the modeled F-16 (using $\bar{q} = 300$, $S = 300$, $b = 30$, $I_{xx} = 9875$), the dimensionalized FOMs are 1.8 radians/sec^2 for the linear model and .64 radians/sec^2 for the nonlinear model. These values match up well to the M1 maneuver, which is a heading change, and the M3 maneuver, which is the climbing turn. The nonlinear model residuals for these two maneuvers are roughly .4 of the linear model. This is slightly worse than the expected improvement of .36 but it is a reasonable result, given that the flight conditions do not match up exactly. For mild maneuvers, the nonlinear model offers a much better prediction of the angular acceleration, pdot.

The expected FOMs do not reflect the larger residuals in Figure 4-1b. However, remember that maneuver M2, the peek and dive, is a more severe maneuver designed to represent evasion level aircraft behavior. A closer inspection of the angle of sideslip for this maneuver (Figure 4-2) will reveal that the aircraft is clearly operating outside the β range that was used to design the models. β was limited to a narrow operating bandwidth of 2.5 degrees during the design process (subsection 4.1.2, step 3) specifically because it displayed very discontinuous properties outside that range, and thus was simplified to a low-ordered polynomial model. As a result, the severe nonlinear characteristics of β contributes to a larger than expected residual for both models in M2. Had time permitted, a piecewise linear approach would have relaxed the requirement for such a narrow limit.

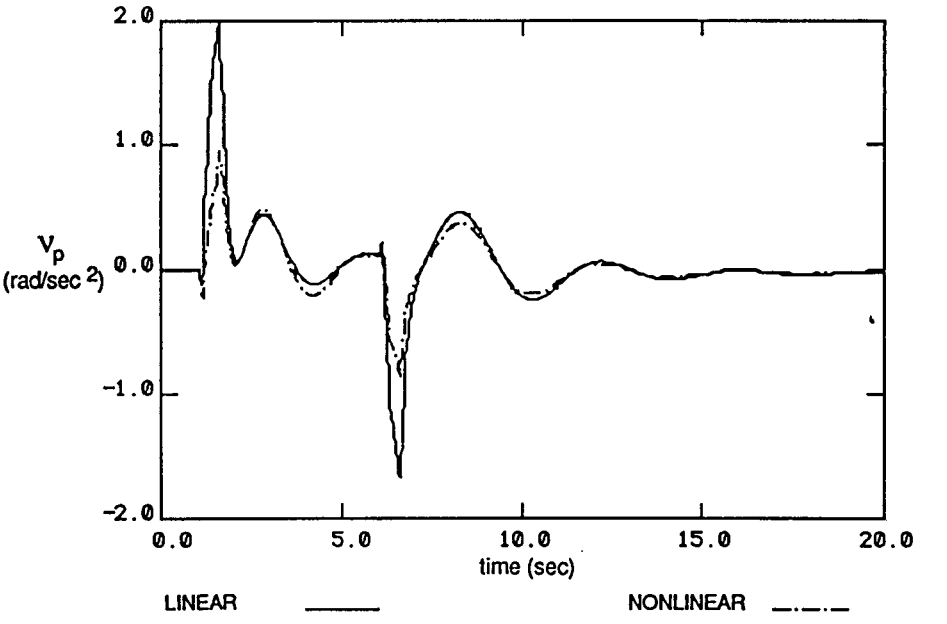

Figure 4-1a. Linear vs. Nonlinear M1 F1.

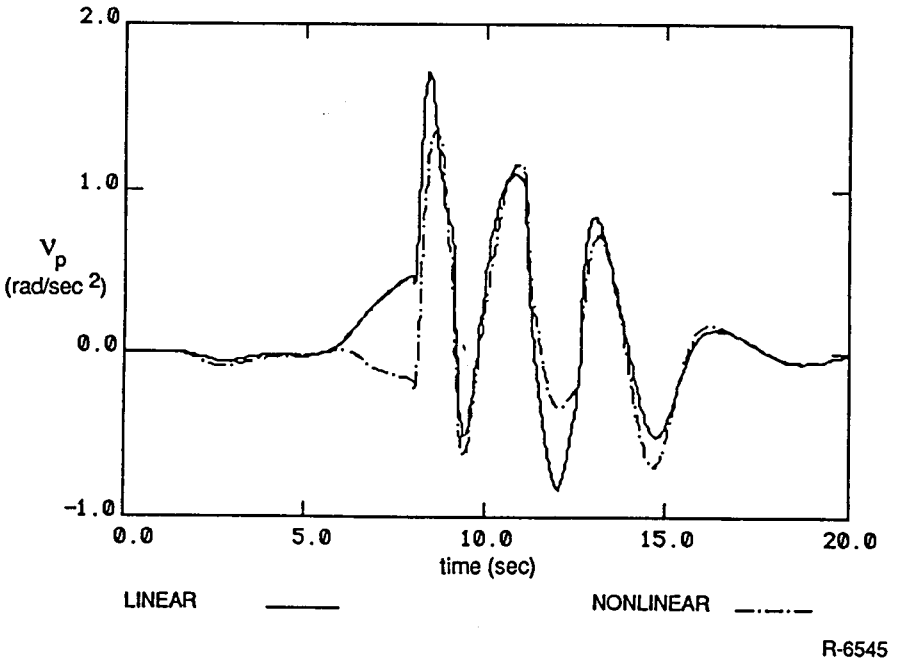

Figure 4-1b. Linear vs. Nonlinear M2 F1.

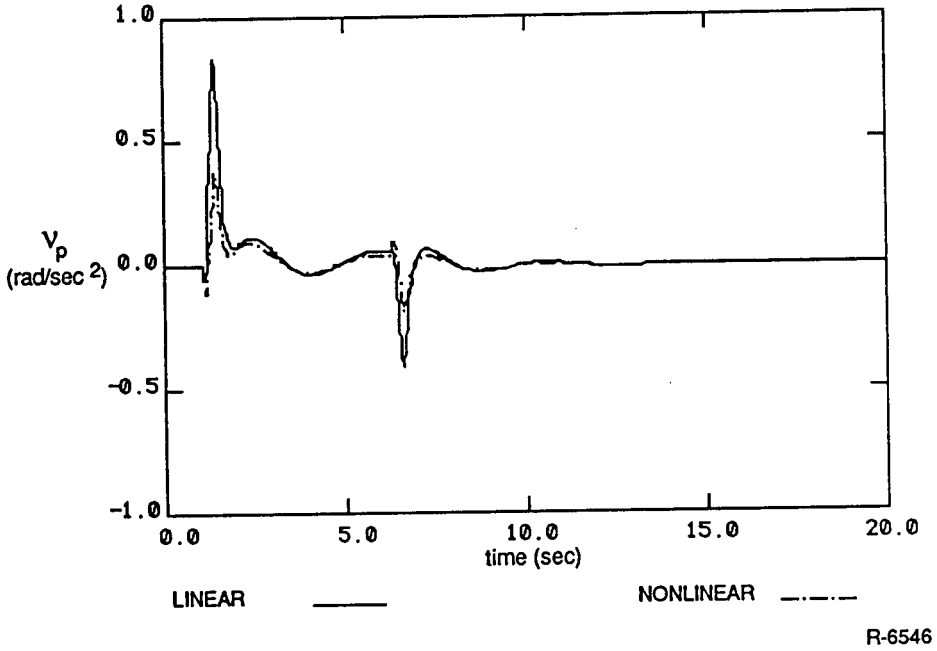

Figure 4-1c. Linear vs. Nonlinear M3 F1.

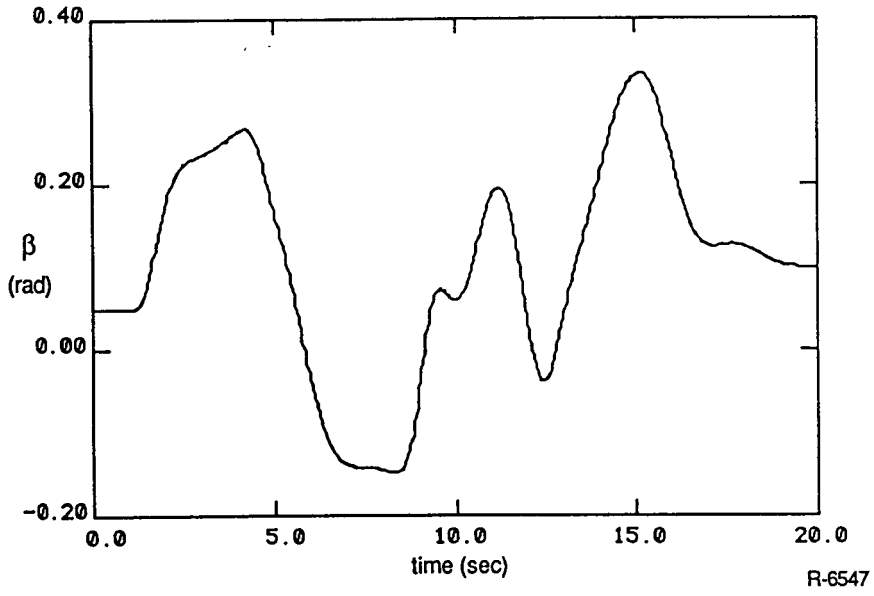

Figure 4-2. Beta for M2 F1.

Backward Elimination Procedure Performance

The backward elimination process was utilized to reduce the number of terms in the original 31-term nonlinear model (Eq. 4-9 from subsection 4.1.2) to a 22-term model (Eq. 4-10 from subsection 4.1.2). It was hypothesized that a reasonable number of terms could be removed without significantly reducing the accuracy of the model. From the Figure Of Merit computations in subsection 4.1.2, the loss in accuracy in switching from the nonlinear 31-term model to the nonlinear 22-term model was slightly greater than one percent of the standard deviation (2.39 E-3 to 2.35 E-3).

Two plots comparing the residuals generated from the nonlinear 31-terms and nonlinear 22-terms models are given in Figure 4-3. For these plots, the flight condition chosen was the same as in the plots above and the input "flight data" was not injected with noise. Since, it was shown that the M2, the peek and dive, is not a representative maneuver given the limit to the sideslip angle range, that maneuver is omitted in the plots. Figure 4-3a compares the two models during the heading change maneuver (M1) and Figure 4-3b compares the two models during the climbing turn maneuver. As expected, Figure 4-3a shows the minimal loss in accuracy from a 31-term nonlinear model to a 22-term nonlinear model. A peculiar result is shown in Figure 4-3b for the M3 maneuver, where it appears that the reduced set of terms actually improves on the accuracy of the residuals. A plausible explanation for this phenomenon is that the 31-term model may be overfitted to the sampled data. The region in which this oddity occurs, between 1.25 seconds and 6.25 seconds, is the period when the aircraft is in a steady climb with no control deflection change or attitude change. Therefore, it is possible that a lower number of terms may better describe a simple motion.

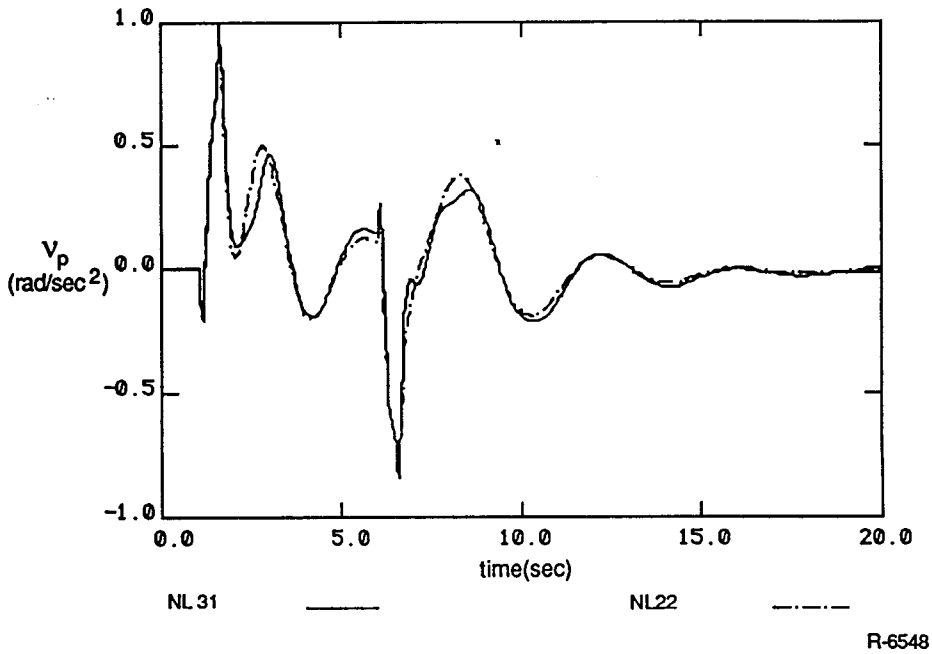

Figure 4-3a. Nonlinear 31 vs. Nonlinear 22 M1 F1.

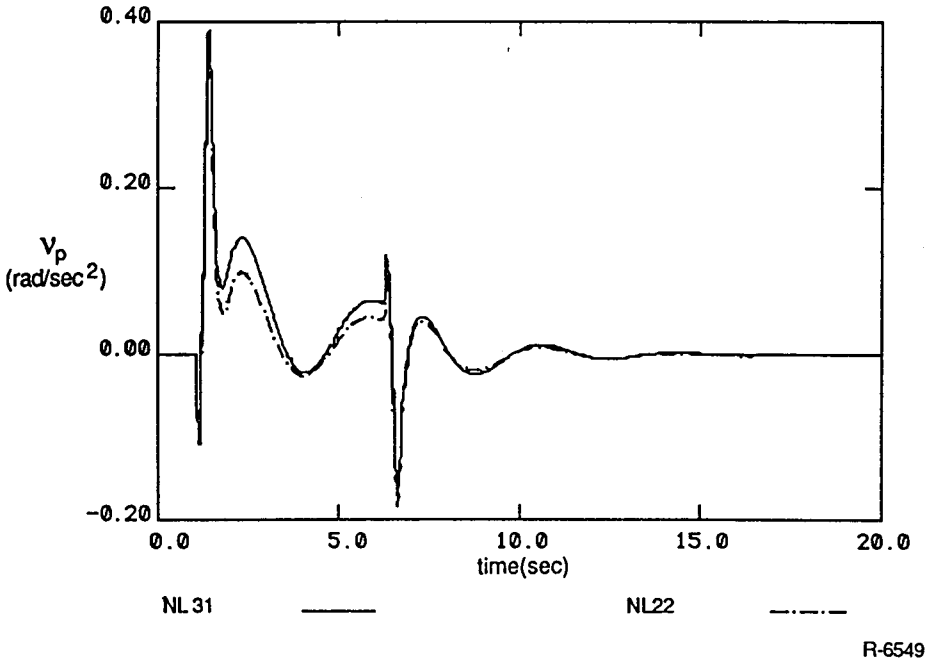

Figure 4-3b. Nonlinear 31 vs. Nonlinear 22 M3 F1.

Residual Mean-Square Minimization Performance

The original intent of incorporating sensor noise computations was to derive the optimal nonlinear model using a sensor noise to modeling noise tradeoff. In addition, models that include sensor noise computations should perform better in the residual generation process than models that don't consider sensor noises, since in real applications, all measurements, by definition, must have some intrinsic noise characteristics.

To test this hypothesis, residuals were generated using a full 31-term nonlinear model without noise computations (Eq. 4-9 from subsection 4.1.2) and a full 31-term nonlinear model with noise computations (Eq. 4-18 from subsection 4.1.3). The 31-term models were selected instead of the 22-term models because the 31-term models include ten terms, that were deemed less significant contributors to modeling given their respective inherent noise values, that the 22-term models do not have. Theoretically, the model with sensor noise computations will downweight these terms more significantly than the model without sensor computations. However, the actual regression coefficients of the two models (with and without sensor computations) are so similar, i.e., less than one percent difference, it is expected that no noticeable difference in the performance of the two models will appear.

For this comparison, maneuver M3, the climbing turn maneuver, was chosen for the same flight condition as for the other runs, namely, F1. The resultant residual for the nonlinear model with sensor noise computation and the model without sensor noise computation are plotted in Figure 4-4a and Figure 4-4b, respectively. As expected, the two plots are almost identical. A closer inspection of the noise computation reveals why this should happen. Recall that the purpose for using this method is to remove terms with large sensor noise relative to its modeling contribution. But if all sensor noises are modeled at the same level (e.g. , all deflections have .1 degree standard deviation) , then they will all have equal weight relative to each other, effectively reducing the problem to one that uses no sensor noise computations. For the case that is modeled here, all Σ values for the individual predictor terms are less than one and are small compared to the range of the predictor terms.

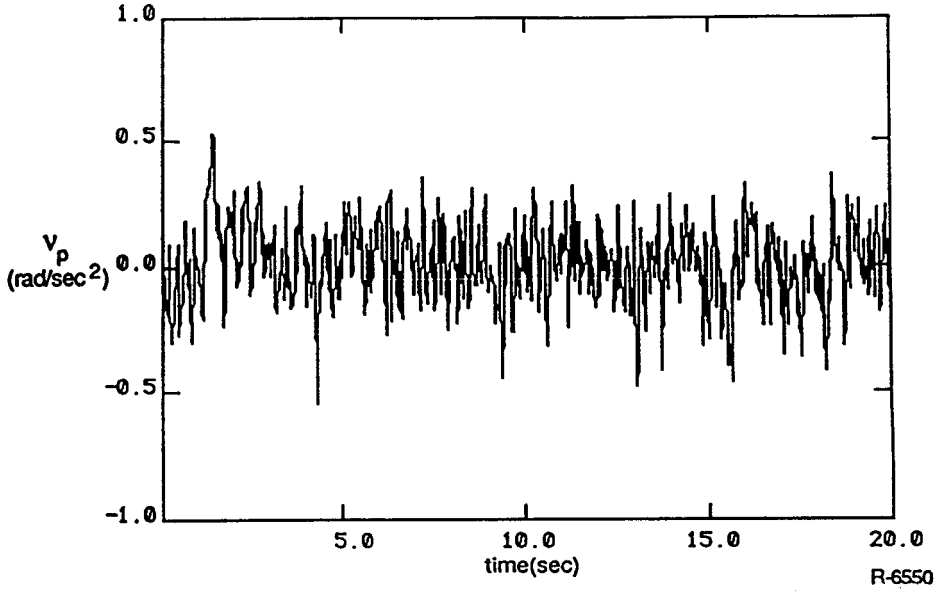

Figure 4-4a. Nonlinear 31 With Sensor Model Noise M3 F1.

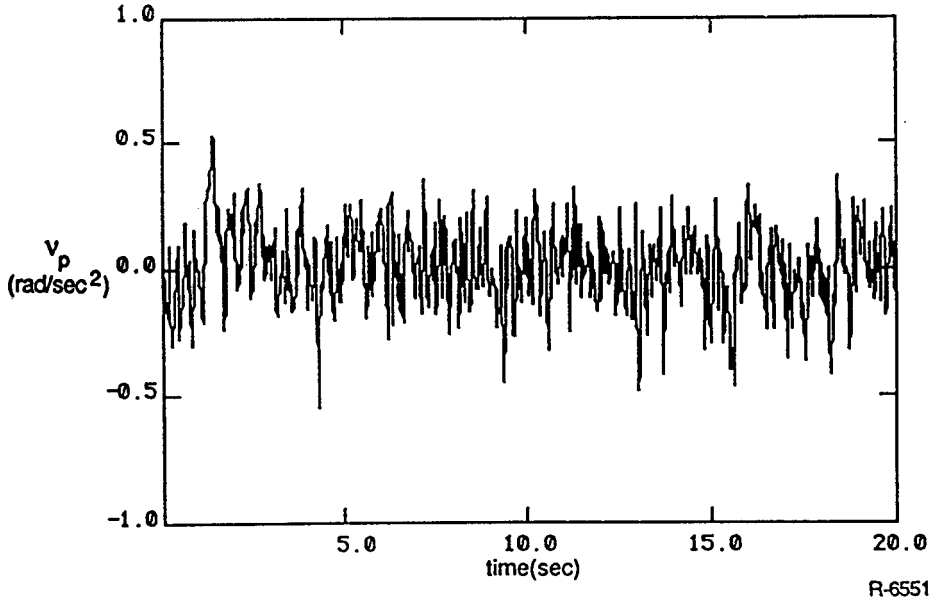

Figure 4-4b. Nonlinear 31 Without Sensor Model Noise M3 F1.

To show that the Σs should not have any effect on the residuals, the following test case was executed. A simple two-term polynomial,

$$y = 4x + 5w$$

was put through the same regression program used for the F-16 models. Ten samples were generated for (x,w) where (x,w) varied from -10. to 10. The first test case used identical Σ values for x and w, namely,

$$\sigma_X = \sigma_W = .01$$

The resulting coefficients from the regression produced $a_X = 3.99$ and $a_W = 4.99$, almost identical to the true values. However, when the Σs are very different, such as,

$$\sigma_X = 60. \qquad \sigma_W = .01,$$

then the value of this method is truly realized. For this case, the x variable has a very high sensor noise compared to its normal range, thus, it is downweighted in the regression . The resulting coefficients for this case are $a_X = 0.301$ and $a_W = 4.318$, reflecting the lack of reliability in the x measurement. The sensors in the F-16 models more resemble the first test case than the second.

Off-Nominal Flight Condition Performance

Originally, the development of the extended envelope residual generation process called for modeling the F-16 with a nonlinear polynomial at multiple flight conditions. The residual generator would then be scheduled across the various flight conditions to provide a more responsive model. However, time constraints did not permit implementation of the full scope of the plan. Using multiple flight conditions necessitates a tighter fit of the flight characteristics for each condition than a method that requires one model to fit all conditions (which must be a more relaxed fit to encompass more possible flight conditions). Therefore, it is not expected that these models, designed for one specific flight condition, would perform well in other flight conditions.

To test the robustness of the models, the nonlinear 22-term model (Eq. 4-10 from subsection 4.1.2) was used at all three flight conditions with the climbing turn maneuver (M3). The results of these runs are plotted together in Figure 4-5. The model performed well not only for F1, but also F2, the low-speed case. However, the model breaks down when tasked to produce residuals for the supersonic case. This is understandable considering that the predictor terms were chosen to characterize the subsonic region of flight, not the highly nonlinear region of supersonic flight.

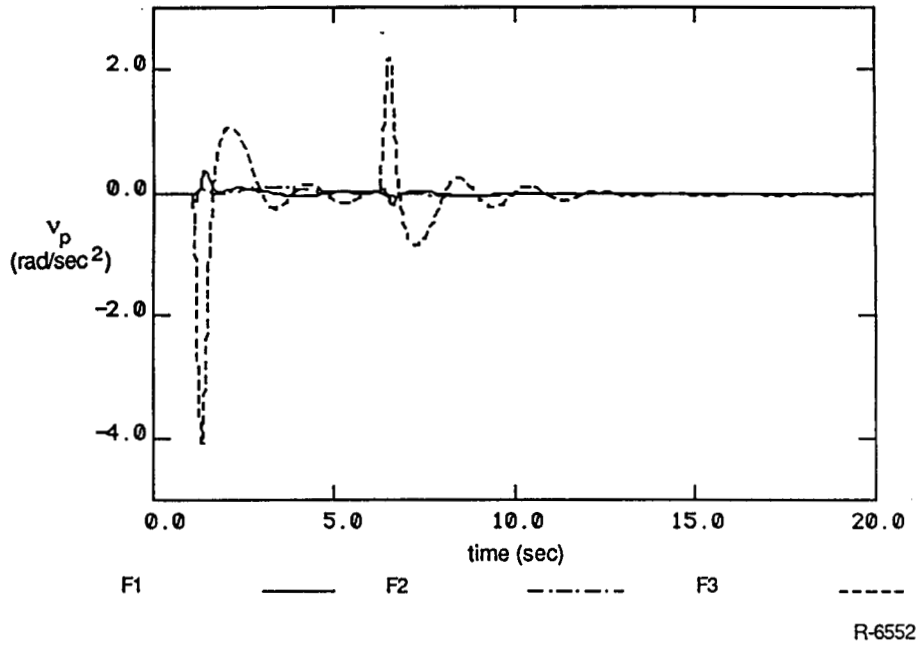

Figure 4-5. Nonlinear 22 at Three Flight Conditions M3 @ F1, F2, F3.

4.2.4 Summary

In this section, a method for developing an extended envelope residual generator has been given. Using backward elimination regression analysis, a non-linear, polynomial model of an AFTI/F-16 is created. Significant effort was placed on deducing the optimal set of predictor terms. In this regard, alternative methods for solving the predictor term problem were also developed, namely, a residual mean-square minimization method that incorporates the use of sensor noise computations. The extended envelope residual generator requires

multiple models for multiple flight conditions. However, time did not permit the development of any additional model. The residual generation results are therefore based on a models developed at a single flight condition.

The nonlinear models performed better than the linear models, as expected. Performance ,however, was constrained by the lack of a perfect match between the flight condition used to design the model and the flight conditions selected for the "flight data". It was also predicted that reducing the original set of nonlinear terms from 31-terms to 22-terms would not significantly detract from the accuracy of the residuals that were generated although significantly simplifying computations. Models developed using sensor noise computations were expected to perform much better than models that did not consider sensor noise computations. However, due to the relatively small sensor noise levels, performance gains were minimal. Finally, the models that were developed were not expected to perform exceptionally well over a wide range of flight conditions since the whole extended envelope approach requires that multiple models, each one tightly fitted to its flight condition, be developed.

Many areas in this method show possibilities for even further accuracy in the residual generation process. First of all, multiple flight conditions must be modeled to insure a truly robust residual generator. Use of the sensor noise computation method should be exploited if sensor noises prove to be high for the aircraft. If sensor noises are relatively low, the backward elimination method is very reliable. The reduction of the number of terms could be carried out even further, given the promising results of almost no lost accuracy for the terms that were removed. Other areas of investigation include the use of a piecewise-linear model to circumvent the discontinuous characteristics of certain predictors, such as β.

SECTION 5

SUMMARY

This report presented the results of an effort to develop envelope-expansion methods for the control element FDI algorithm developed in [2]. As in past efforts, this effort was divided into two related tasks, residual generation and decisionmaking design. Separate consideration of these aspects of the FDI problem allows accountability for many of the non-idealized effects that make the FDI problem most difficult. This effort assumed that the structure of the FDI algorithm would be predetermined and that adaptation of its parameters as a function of the appropriate flight condition values is required.

For residual generation, the adaptation mechanism we considered is a model scheduling mechanism as opposed to a model "learning" mechanism to avoid the problem of false adaptation to the failures we wish to detect. Effects that need to be considered include both large-amplitude maneuvers and changes due to Mach and altitude. The effect of large maneuvers at a single flight condition involves nonlinearities and interactions that are normally not considered in a linear aerodynamic model (e.g., for control design). Significant changes may also occur as a function of Mach and altitude because of the flexibility of the aircraft and the effect on load distributions due to flight condition. Qualitative prediction of the large maneuver effects is possible through physical arguments involving standard aerodynamic concepts. The so-called "static flexibility" effects are less understood and, therefore, require explicit scheduling using look-up tables.

For large maneuver effects, the scheduling is accomplished "implicitly" by construction of an analytic nonlinear model. This model is derived as a simplification to a mature aero package, although advanced identification techniques could be directly applied to flight test data as well. The development of a useful nonlinear model for the residual generation process

should incorporate physical understanding of aerodynamics (to avoid complex and/or overfitted models) and must consider the effects of sensor noise in determining the utility of individual elements of the model. Physical understanding led to a "panel method" model format. This format, however, had several drawbacks and led to the consideration of a quasi-linear model. This model assumes the form of a linear aerodynamic model, but with "derivatives" that are modeled as a function of other variables. The selection of which variables influence which "derivatives" is then justified from a physical standpoint. When the quasi-linear model is further expanded into a "parameter-linear" format, regression analysis can be used to estimate the best set of parameters. We then derived a small modification to standard regression methods that explicitly deal with sensor errors in determining optimal residual generation parameters.

For decisionmaking (DM), we also assumed that the temporal characteristics (i.e., spectral shape) of the residuals are constant so that filtering requirements for each hypothesis test do not need to be scheduled. Scheduling of DM parameters is potentially required whenever changes to the covariance of the filtered residuals occur and whenever changes to the failure directions occur. The former requires changes to both thresholds and projection vectors while the latter only requires changes to projection vectors. Although failure directions may change whenever the control derivatives change, if these changes effect all derivatives in a similar manner, then the failure directions remain constant. When all derivatives are not affected in a similar manner, scheduling of the projection vectors must occur. However, this is only possible if the parameters affecting the failure directions are measurable. Such is not the case when a failure direction is affected by its corresponding control element value. Should this occur (as it does for the flaperons on the F-16) care must be taken in the design of tests for flaperon failures (particularly in using the pitching-moment residual).

The measurable quantities upon which scheduling must be based include dynamic pressure, roll rate, and angle of attack, since their values have a direct impact on the sensor noise component of the residuals. However, other effects, such as those that are modulated by

maneuver size are more difficult to describe. One way to establish scheduling requirements for these effects is to perform an empirical study (using either a high-fidelity simulation or flight-tests) and to schedule parameters as a function of the "size" of aircraft "inputs."

Once the flight-condition parameters are defined, the DM design goal becomes one of balancing complexity and performance of the scheduling mechanism. The simplest DM design is a fixed-parameter solution and should be used if its performance is adequate. At the other extreme is a DM design in which all parameters must be scheduled. In between these extremes a partial fixed/variable design allows for some parameters to be fixed and some to vary as a function of flight condition. Design and evaluation methods were given for all three DM-design concepts.

In application of residual-generation methods to the AFTI-F-16, the nonlinear models performed better than the linear models, as expected. Performance ,however, was constrained by the lack of a perfect match between the flight condition used to design the model and the flight conditions selected for the "flight data". It was also predicted that reducing the original set of nonlinear terms from 32-terms to 22-terms would not significantly detract from the accuracy of the residuals that were generated although significantly simplifying computations. Models developed using sensor noise computations were expected to perform much better than models that did not consider sensor noise computations. However, due to the relatively small sensor noise levels, performance gains were minimal. Finally, the models that were developed were not expected to perform exceptionally well over a wide range of flight conditions since the whole extended envelope approach requires that multiple models, each one tightly fitted to its flight condition, be developed.

Many areas in this method show possibilities for even further accuracy in the residual generation process. First of all, multiple flight conditions must be modeled to insure a truly robust residual generator. Use of the sensor noise computation method should be exploited if sensor noises prove to be high for the aircraft. If sensor noises are relatively low, the backward elimination method is very reliable. The reduction of the number of terms could be

carried out even further, given the promising results of almost no lost accuracy for the terms that were removed. Other areas of investigation include the use of a piecewise-linear model to circumvent the discontinuous characteristics of certain predictors, such as β.

APPENDIX A

REPRESENTATIVE AERODYNAMIC INTERACTIONS

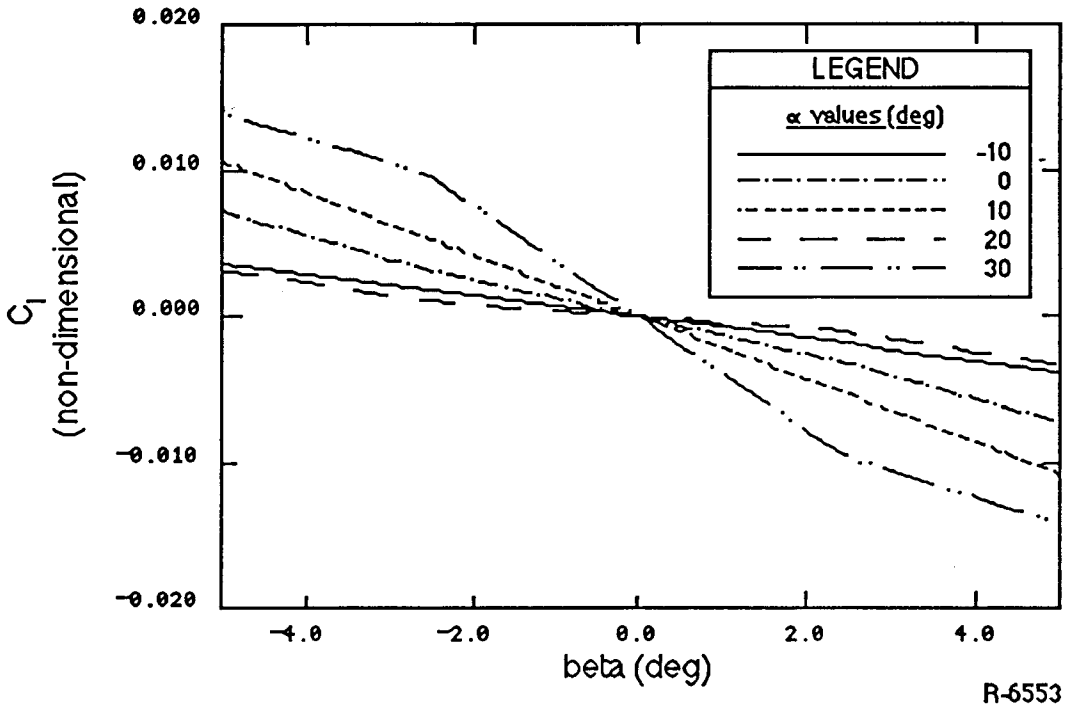

Figure A-1. Sensitivity of C_l to β for Various Values of α.

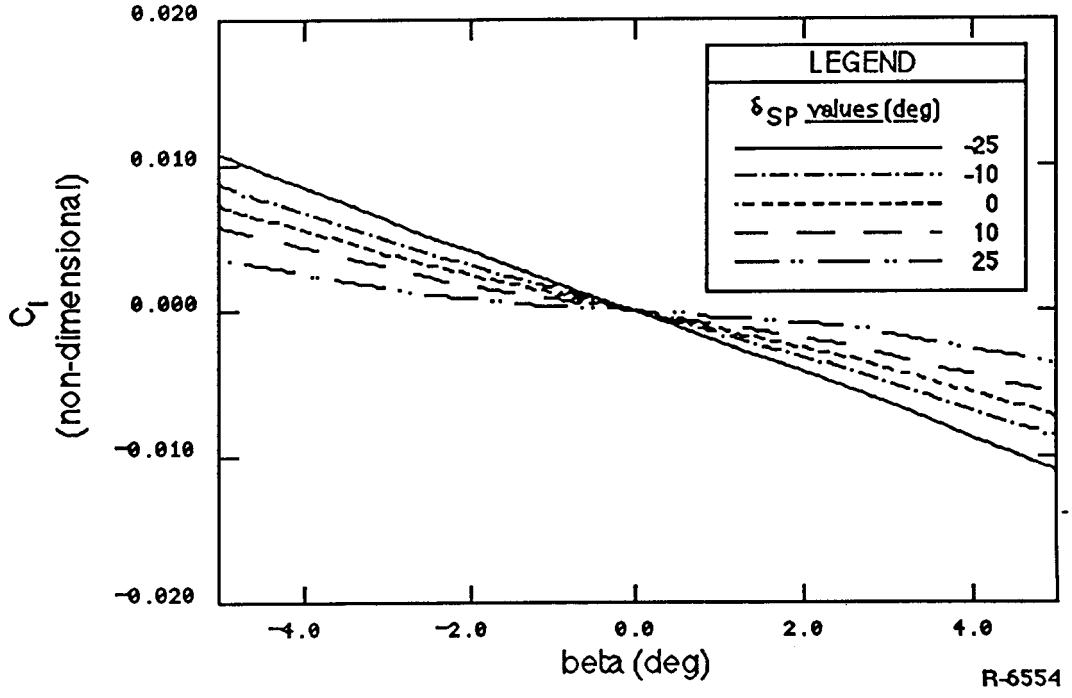

Figure A-2. Sensitivity of C_l to β for Various Values of δ_{SP}.

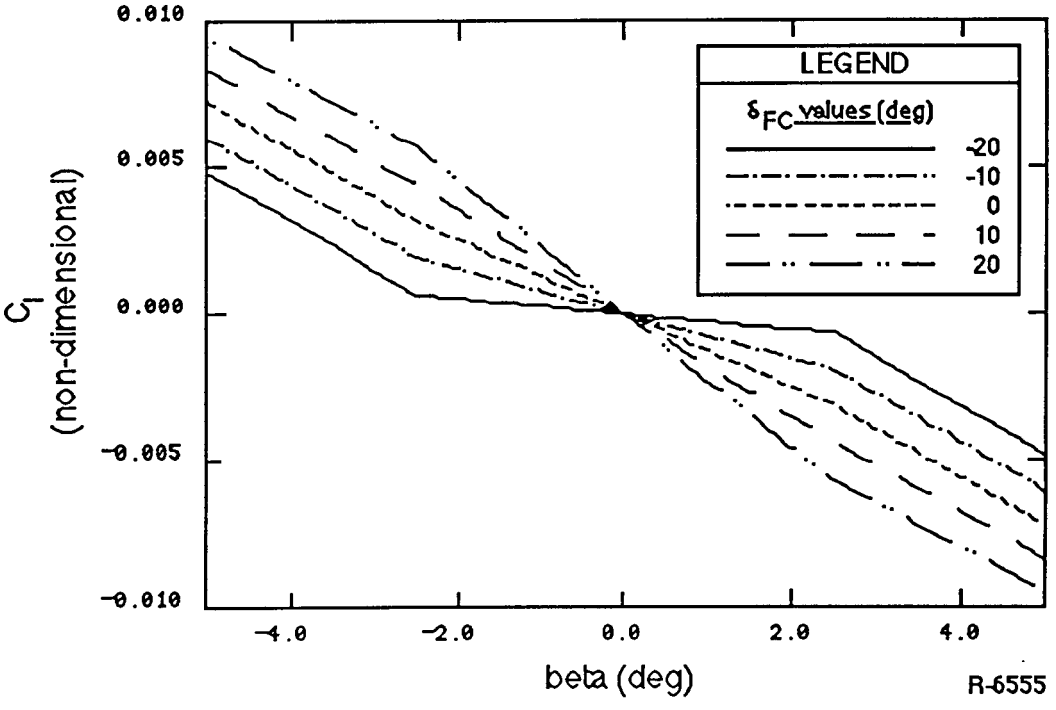

Figure A-3. Sensitivity of C_l to β for Various Values of δ_{FC}.

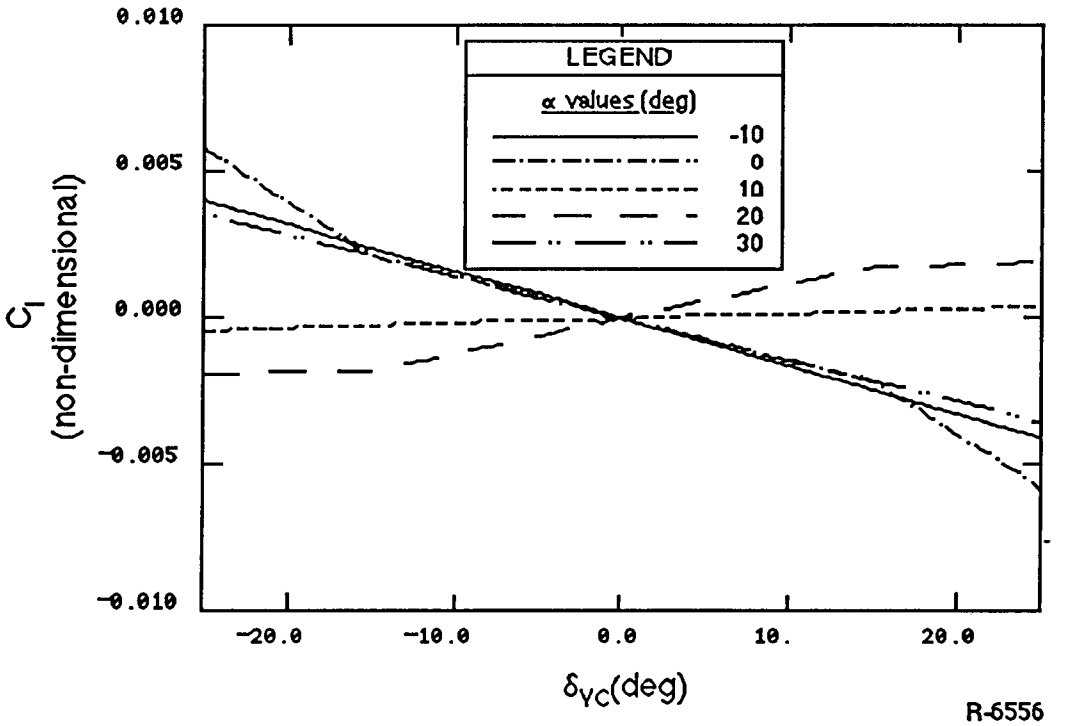

Figure A-4. Sensitivity of C_l to δ_{YC} for Various Values of α.

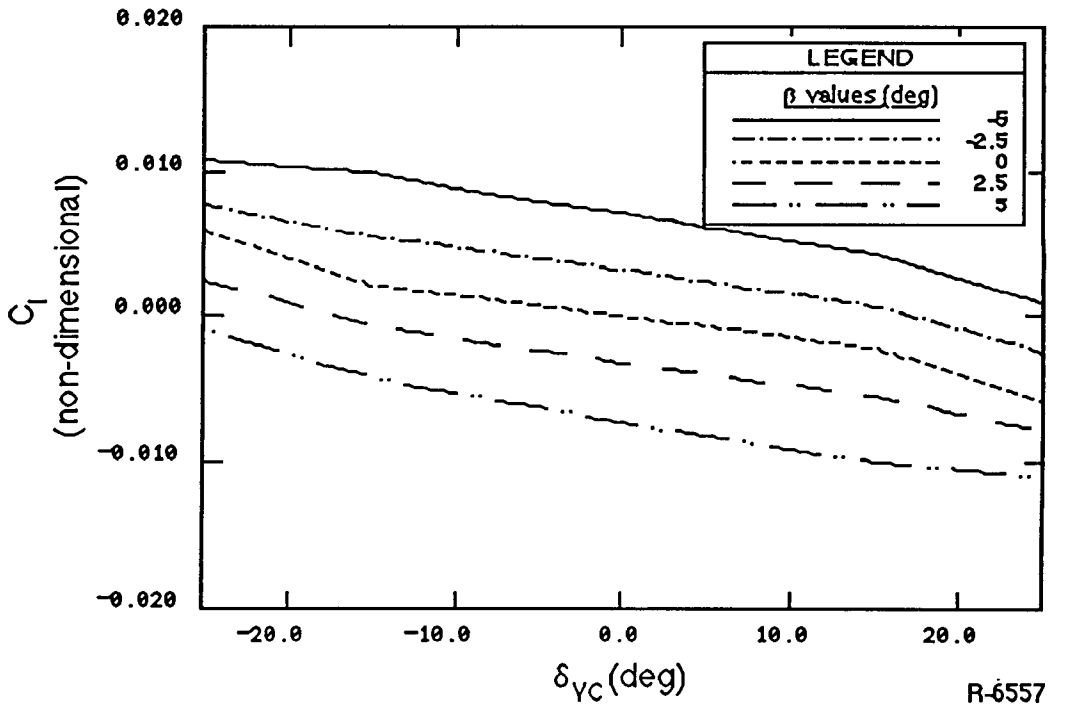

Figure A-5. Sensitivity of C_l to δ_{YC} for Various Values of β.

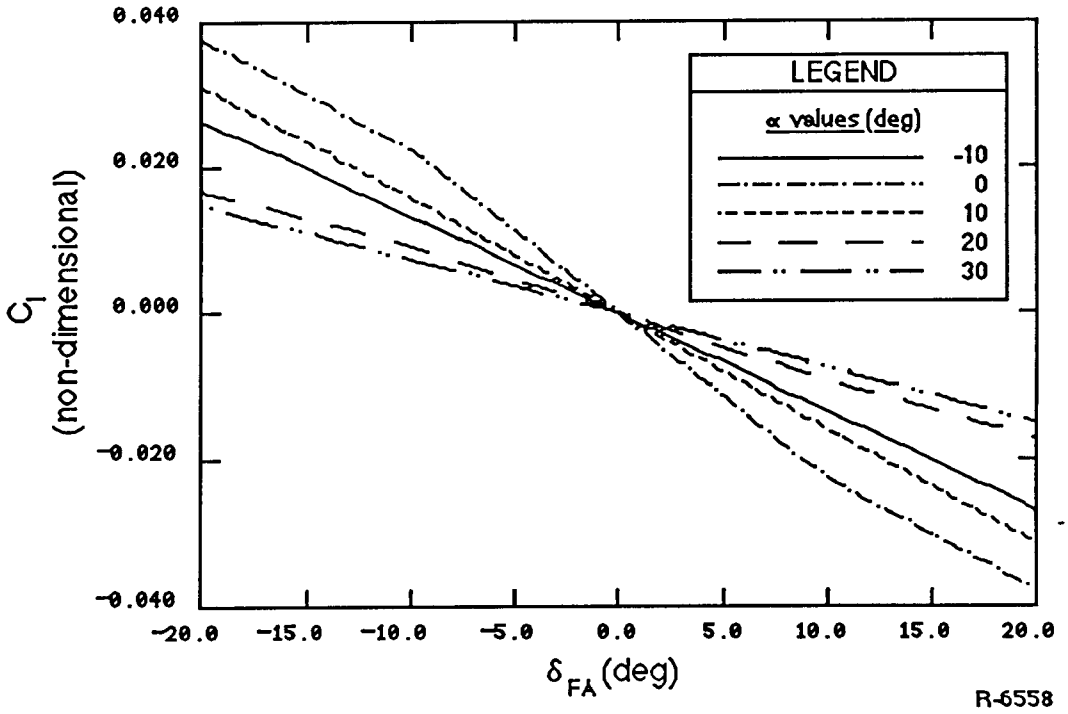

Figure A-6. Sensitivity of C_l to δ_{FA} for Various Values of α.

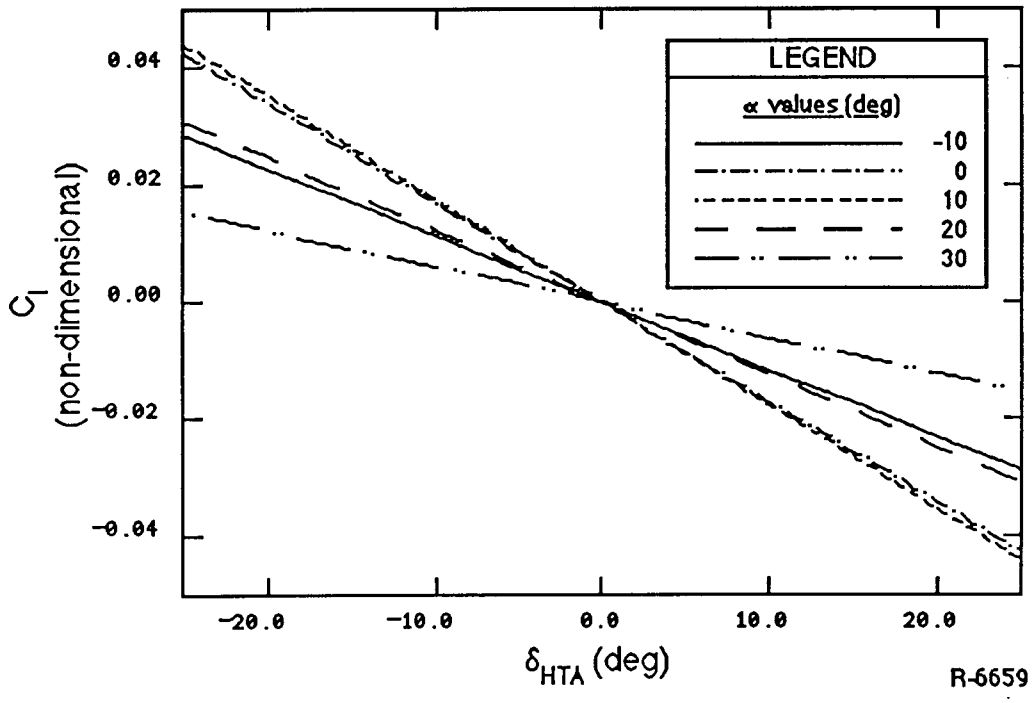

Figure A-7. Sensitivity of C_l to δ_{HTA} for Various Values of α.

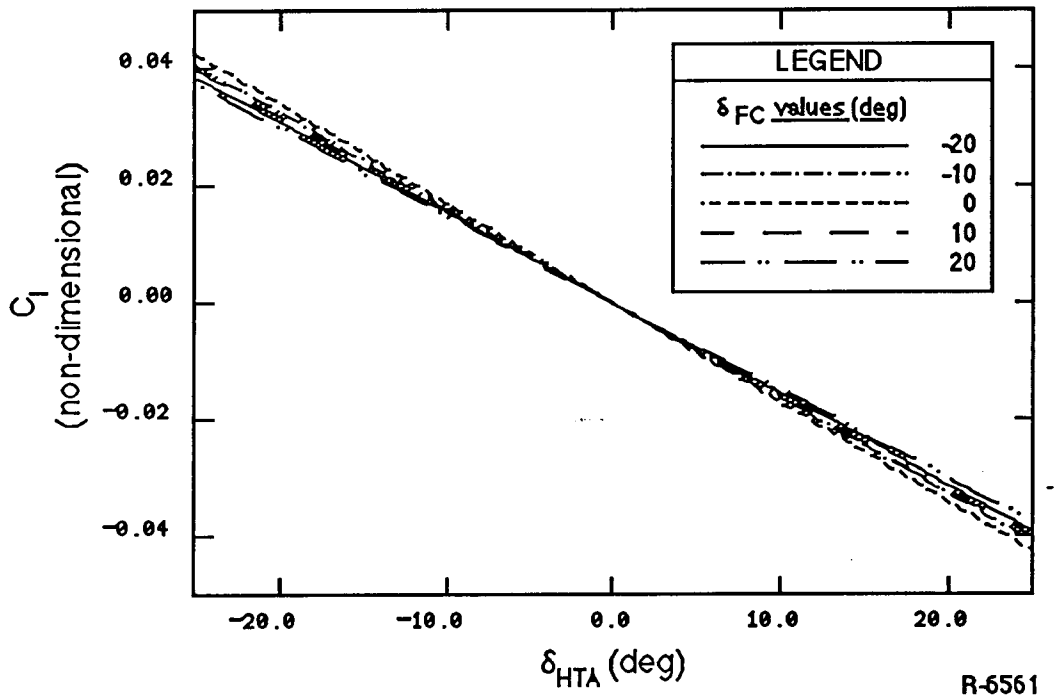

Figure A-8. Sensitivity of C_l to δ_{HTA} for Various Values of δ_{FA}.

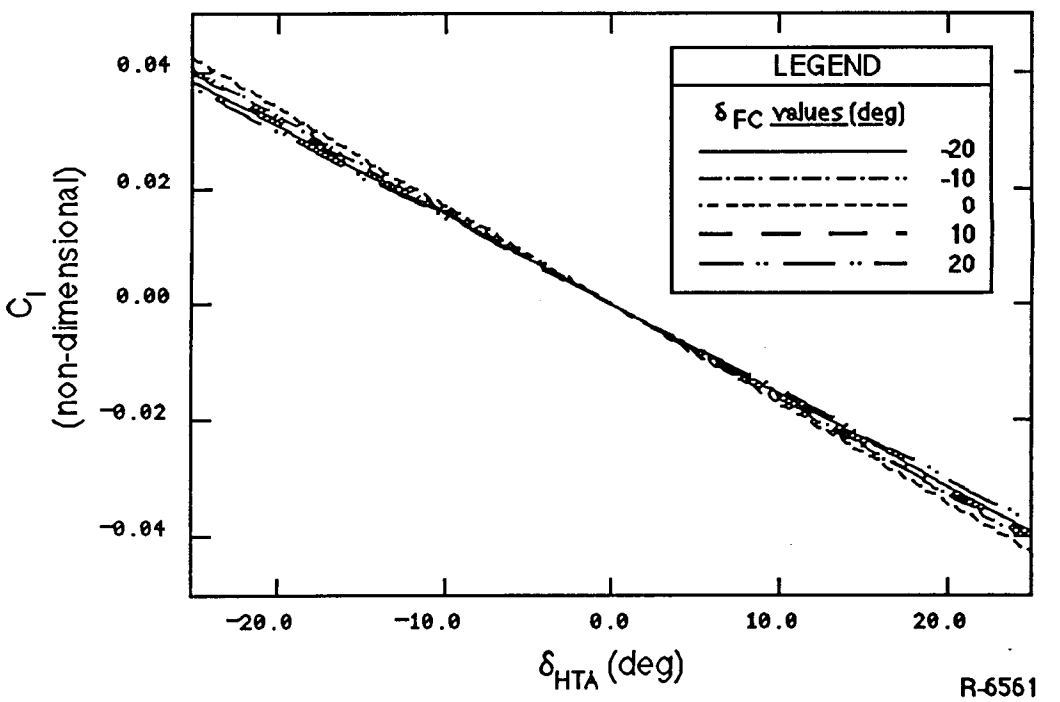

Figure A-9. Sensitivity of C_l to δ_{HTA} for Various Values of δ_{FC}.

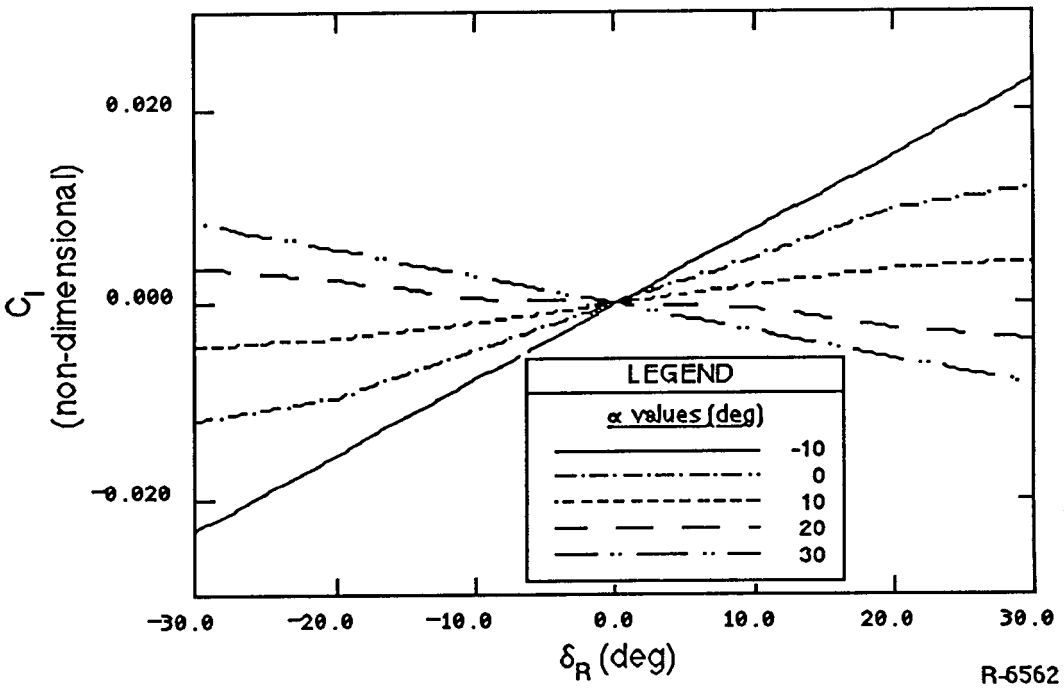

Figure A-10. Sensitivity of C_l to δ_R for Various Values of α.

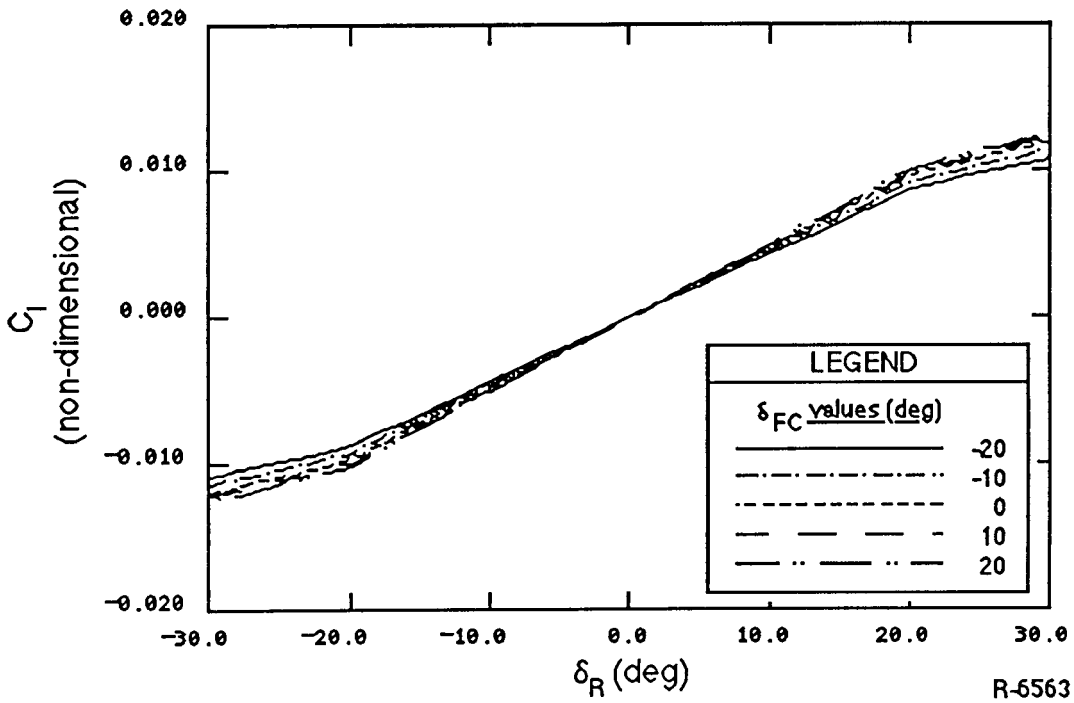

Figure A-11. Sensitivity of C_l to δ_R for Various Values of δ_{FC}.

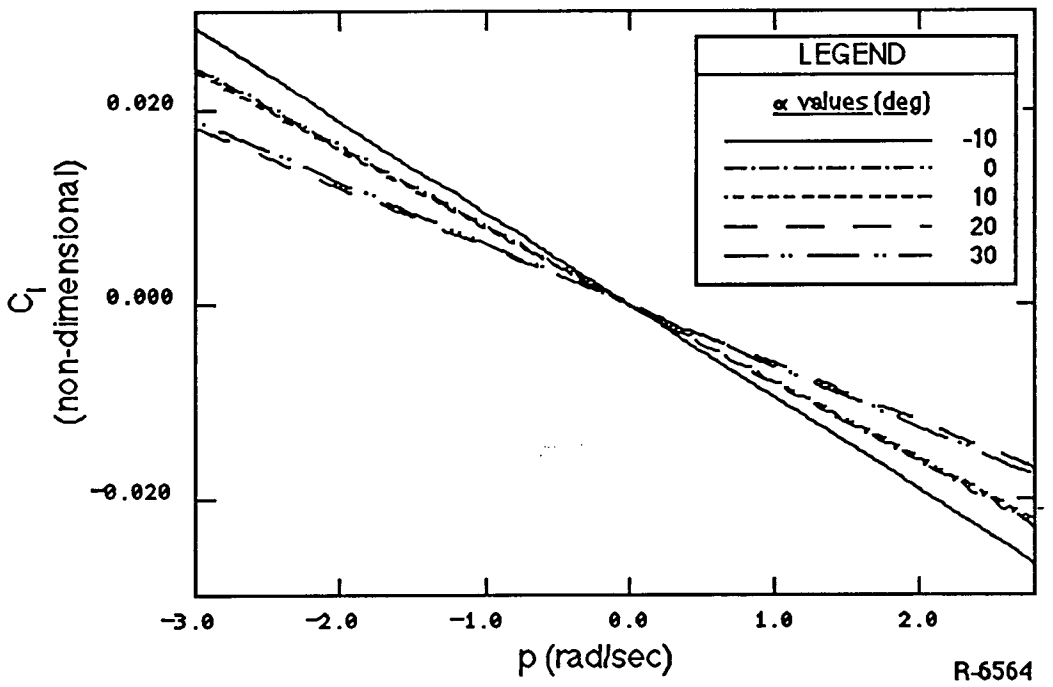

Figure A-12. Sensitivity of C_l to p for Various Values of α.

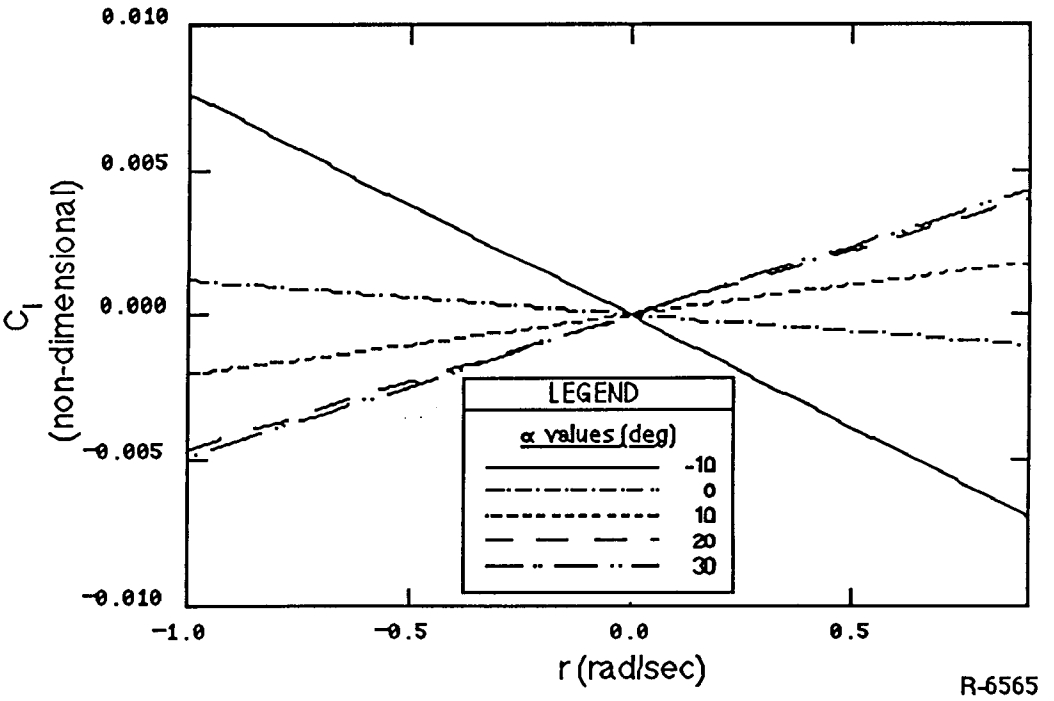

Figure A-13. Sensitivity of C_l to r for Various Values of α.

APPENDIX B

SIMPLIFICATION OF THE DECISION MECHANISM

The decision mechanism developed in [2] required pairwise comparisons of all failure modes implied by the set of trigger results. In the worst case, tests that compare all pairs of failure hypotheses would need to be performed. For very large numbers of failures, such a methodology is computationally infeasible. Reduction of the number of hypothesis tests for large problems is, therefore, desirable. However, since the pairwise methodology ensures large sensitivity to each failure mode, it is expected that fewer tests will result in decreased performance. Nevertheless, the results of [1] suggest that there is substantial room for FDI performance degradation without overall degradation of the restructurable control system of which the FDI algorithm is a part.

One of the critical features of the FDI algorithm in [2] is the use of a sequential test strategy for the individual hypothesis tests that comprise the DM. This strategy allows the system to respond at a speed that is proportional to the size of a failure without compromising false alarm performance. Thus fixed sample size tests such as those used in the "decision-function" approach described in [13] are not of interest. To obtain a "proportional response" sequential tests or multiple window tests must be used. In either case, the DM contains individual tests that "fire" (i.e., pass or fail) asynchronously. Thus the DM must be able to "reason" about test results as they occur or, as in [1] and [2], provide a mapping from the set of possible test results to the set of final decisions.

To establish the framework for a DM that can utilize fewer individual hypothesis tests, we need to define a "reasoning" methodology for the DM to use in its interpretation of test results. Analysis of the overall DM can then, theoretically, be obtained through analysis of all possible combinations of test results and the resulting decisions that can be made (note that in

[2] the mapping from test results to decisions was many to one, thereby allowing aggregation of many test result combinations in the calculation of overall performance).

The interpretation of individual test results in terms of overall decisions is a problem in distributed decisionmaking. Such problems are very difficult as outlined in [14], although many special cases have simple solutions [15]. For the FDI problem, the key information about individual tests that must be available to the DM for test interpretation is the conditional likelihoods defined by:

$$p(T_i \text{ fails} \mid H_j, f_j) \tag{5-1}$$

and

$$p(T_i \text{ passes} \mid H_j, f_j)\,, \tag{5-2}$$

where H_j, f_j indicates that failure mode j occurred with a failure "magnitude" f_j. From this basic information, Bayes rule can be applied as in [15] to obtain the posterior probability density function of f_j for all j (conditioned on a specific set of test results). If the tests are designed properly, then the posterior distributions will indicate that only one failure mode has a significant probability of failure when that failure has actually occurred.

For example, the pairwise tests in [2] can be ideally interpreted by the following:

1. Test T_{ij} failing implies that $f_j = 0$, and for $k \neq j$, $|f_k| > f_k^{ij} > 0$
2. Test T_{ij} passing implies that $f_i = 0$, and for $k \neq i$, $|f_k| > f_k^{ij} > 0$

Note that the tests are designed so that f_j^{ij} is smaller than any other f_j^{kl} $(k, l \neq j)$ and similarly for f_i^{ij}. When a set of tests pass and fail, the distribution of each f_k is given by the intersection of the real line sets implied by applying 1 and 2. Thus, if failure i occurs, and all tests T_{ij} $(j \neq i)$ fail, then the only failure mode with a nonzero "signature-set" is f_i. Equations 5-1 and 5-2 are simply probabilistic descriptions of the test interpretations described above.

Now, with this method of interpreting tests, we can envision a design process that creates tests and the information in the form of Eqs. 5-1, 2 for each test. Analysis of all interpretations of all test results can then be made and from this, the mapping from individual test results to final failure decisions can be created.

REFERENCES

[1] Weiss, J., D. Looze, J. Eterno, and D. Grunberg, "Initial Design and Evaluation of Automatic Restructurable Flight Control System Concepts," NASA CR-178064, June 1986.

[2] Weiss, J. and J. Hsu, "Design and Evaluation of a Failure Detection and Isolation Algorithm for Restructurable Control Systems," NASA CR-178213, March 1987.

[3] Weiss, J. and J. Hsu, "Integrated Restructurable Flight Control System Demonstration Results," NASA CR-178305, May 1987.

[4] Huber, R. and B. McCullough, "Self-Repairing Flight Control Systems, Society of Automotive Engineers, Paper #SAE-841552, presented at Aerospace Congress and Exposition, Long Beach, CA, October 1984.

[5] Draper, N., Smith, H., Applied Regression Analysis, 2nd Ed., John Wiley & Sons, 1981.

[6] Roskam, J., Airplane Flight Dynamics and Automatic Flight Controls, Univ. of Kansas, Part 1, 1979.

[7] Etkin, B., Dynamics of Atmospheric Flight, Wiley and Sons, NY, 1972.

[8] Klein, V., "Determination of Airplane Model Structure From Flight Data by Using a Modified Stepwise Regression", NASA TP-19116, Oct. 1981.

[9] Weiss, J.L., K.R. Pattipati, et al., "Robust Detection and Isolation of Sensor Failures", NASA CR 174797, September 1985.

[10] McRuer, D., Ashkenas, I., Graham, D., Aircraft Dynamics and Automatic Control, Princeton University Press, 1973.

[11] Law, A.M., Kelton, W.D., Simulation Modeling and Analysis, McGraw-Hill Book Company, 1982.

[12] Strang, G., Linear Algebra and Its Applications, Academic Press, 1976.

[13] Daly, K., et al., "Generalized Likelihood Test for FDI in Redundant Sensor Configurations," J. Guidance and Control, Vol. 2, No. 1, Jan.-Feb. 1979.

[14] Tsitsiklis, J.N. and M. Athans, "Convergence and Asymptotic Agreement in Distributed Decision Problems," IEEE Transactions on Automatic Control, 1984.

[15] Tenney, R. and N.R. Sandell, Jr., "Detection with Distributed Sensors," IEEE Transactions on Aerospace and Electronic Systems, Vol. AES-17, No. 4, 1981.

NASA National Aeronautics and Space Administration

Report Documentation Page

1. Report No.	2. Government Accession No.	3. Recipient's Catalog No.
NASA CR-181664		

4. Title and Subtitle	5. Report Date
Expanded Envelope Concepts for Aircraft Control-Element Failure Detection and Identification	June 1988
	6. Performing Organization Code

7. Author(s)	8. Performing Organization Report No.
Jerold L. Weiss and John Y. Hsu	TR-378
	10. Work Unit No.
	505-66-01-02

9. Performing Organization Name and Address	11. Contract or Grant No.
ALPHATECH, Inc. 2 Burlington Executive Center 111 Middlesex Turnpike Burlington, MA 01803	NAS1-18004
	13. Type of Report and Period Covered
	Contractor Report

12. Sponsoring Agency Name and Address	14. Sponsoring Agency Code
National Aeronautics and Space Administration Langley Research Center Hampton, VA 23665-5225	

15. Supplementary Notes

Langley Technical Monitor: W. Thomas Bundick
Final Report

16. Abstract

The purpose of this effort was to develop and demonstrate concepts for expanding the envelope of failure detection and isolation (FDI) algorithms for"aircraft-path" failures. The previously developed FDI algorithm, which uses analytic-redundancy in the form of aerodynamic force and moment balance equations, was used as a basis for this study. Because aircraft-path FDI uses analytical models, there is a tradeoff between the accuracy of these models and the ability to detect and isolate failures. For single flight condition operation, we developed design and analysis methods to deal with this "robustness" problem. When the departure from the single flight condition is significant, however, it is not possible to obtain adequate performance (i.e., both low false alarm and missed detection probabilities) without some form of algorithm adaptation. Adaptation requirements for the residual generation portion of the FDI algorithm are interpreted as the need for accurate, large-motion aero-models, over a broad range of velocity and altitude conditions. For the decision-making part of the FDI algorithm, adaptation may require modifications to filtering operations, thresholds, and projection vectors that define the various hypothesis tests performed in the decision mechanism. Methods of obtaining and evaluating adequate residual generation and decision-making designs have been developed in this project. In addition, we have demonstrated the application of the residual generation ideas to a high-performance fighter by developing "adaptive" residuals for the AFTI-F-16 and simulating their behavior under a variety of maneuvers using the results of a NASA F-16 simulation.

17. Key Words (Suggested by Author(s))	18. Distribution Statement
FDI, Failure Detection, Analytic Redundancy, Extended Flight Envelope	Unclassified - Unlimited Subject Category 04

19. Security Classif. (of this report)	20. Security Classif. (of this page)	21. No. of pages	22. Price
Unclassified	Unclassified	99	

NASA FORM 1626 OCT 86